Turbulence in binary fluid mixtures

Ricardo Ruiz
Department of Physics, Massachusetts Institute of Technology, Cambridge, Massachusetts 02139

David R. Nelson
Department of Physics, Harvard University, Cambridge, Massachusetts 02138

(Received 1 December 1980)

Turbulence in binary fluid mixtures is studied. Because concentration gradients can react back on the advecting velocity field, such systems support (overdamped) transverse waves. The primary effect of this coupling in miscible high-Prandtl-number fluids is to shorten the viscous-convective cascade of concentration fluctuations. When concentration fluctuations are injected at short wavelengths, we find at time-dependent inverse cascade with spectrum $C(k) \sim k^{-7/3}$. This cascade may be related to the dynamics of phase-separating binary mixtures at intermediate times.

I. INTRODUCTION

A. Purpose

A salient feature of turbulent fluid motion is a striking enhancement of transport coefficients.[1] The famous turbulent cascade of velocity fluctuations to small length scales proposed by Kolmogorov in 1941 (Ref. 2) dissipates energy very efficiently. One can define an effective "eddy viscosity" in a chaotic fluid which is orders of magnitude larger than the equilibrium shear viscosity.[1] The turbulent advection of temperature fluctuations and passive contaminants has also received much attention.[3-8] Let us consider for concreteness a mass density $\rho(\vec{r}, t)$ of contaminant liquid molecules, and focus on a dimensionless deviation,

$$\psi(\vec{r}, t) = [\rho(\vec{r}, t) - \rho_0]/\rho_0 , \tag{1.1}$$

from the homogeneous state $\rho(\vec{r}, t) = \rho_0$. We assume the contaminant liquid is miscible with its host. If the host fluid is at rest, $\psi(\vec{r}, t)$ simply diffuses,

$$\partial_t \psi = D\nabla^2 \psi . \tag{1.2}$$

Since typical diffusion constants D are of order 10^{-5} cm^2/sec, a one-centimeter inhomogeneity in $c(\vec{r}, t)$ would relax to uniformity in a time of order one day. Stirring reduces this time drastically, effectively enhancing D by a factor $\sim 10^5$.[1]

"Passive" diffusion or advection of a contaminant correctly describes the dynamics in a relatively small region of the phase diagram for a symmetric AB binary mixture shown in Fig. 1. Below a critical temperature T_c, such systems phase separate into distinct A-rich and B-rich components. Advection of "passive" contaminants takes place on the extreme right and left of this phase diagram, upon stirring. Turbulence in these regimes can be qualitatively understood via a standard phenomenology[3-8] reviewed below. Our aim here is to investigate turbulent transport in, say, 50-50 concentrations of AB binary fluid mixtures. As we shall see, new dynamical effects arise, since concentration fluctuations now react back on the advecting velocity field. Spatially nonuniform but miscible "active" mixtures can respond to stirring rather differently than in the passive case.

Miscible binary mixtures only exist outside the region of two-phase coexistence shown in Fig. 1. Fascinating questions arise when mixtures are stirred violently within this miscibility gap. Presumably, a steady state develops, controlled by turbulent mixing and the contravening tendency of the mixtures to phase separate. Concentration fluctuations in such a nonequilibrium steady state

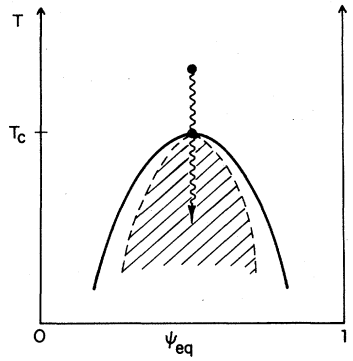

FIG. 1. Schematic plot of the temperature-concentration plane for a symmetric binary mixture in thermodynamic equilibrium. The solid curve bounds a region of two-phase coexistence. The dashed, spinodal curves enclose a shaded region where the effective diffusion constant is negative. An abrupt quench in temperature into this unstable region is shown. The mixture consists primarily of species A on the extreme left, and of species B on the extreme right. Here, the variable ψ_{eq} is $\psi_{eq} = \langle \rho_B(\vec{r}, t) \rangle / \rho_0$.

could be studied with light-scattering techniques, similar to those used to investigate spinodal decomposition.[9] Processes discussed here, which drive miscible binary mixtures toward uniformity, must certainly play a role in turbulent immiscible mixtures as well. Our study of turbulent miscible mixtures may be viewed as a prelude to an attack on this more difficult problem. Some comments and speculations concerning turbulence in phase-separating binary mixtures may be found in the concluding section.

B. Passive versus "active" binary mixtures

In the presence of an advecting macroscopic velocity field $\vec{v}(\vec{r},t)$, the diffusion equation (1.2) for a *passive* contaminant becomes

$$D_t\psi \equiv (\partial_t + \vec{v}\cdot\vec{\nabla})\psi = D\nabla^2\psi . \tag{1.3}$$

The velocity itself obeys the Navier-Stokes equations

$$(\partial_t + \vec{v}\cdot\vec{\nabla})\vec{v} = -\frac{1}{\rho_0}\vec{\nabla}p + \nu\nabla^2\vec{v} + \vec{f} , \tag{1.4a}$$

$$\vec{\nabla}\cdot\vec{v} = 0 , \tag{1.4b}$$

where $\vec{f}$ is a random force stirring the fluid, and Eq. (1.4b) enforces the constraint of incompressibility. To determine how the chaotic velocity field produced by $\vec{f}$ affects the concentration,[3-8] consider the spatial integral of its autocorrelation

$$C_{\rm tot}(t) \equiv \tfrac{1}{2}\int d^3r[\psi(\vec{r},t)]^2 , \tag{1.5}$$

which is conserved in the absence of diffusion,

$$\frac{dC_{\rm tot}(t)}{dt} = -D\int d^3r\,|\vec{\nabla}\psi(\vec{r},t)|^2 . \tag{1.6}$$

Since D is small in typical fluids, rapid mixing can only be achieved if stirring produces large concentration gradients. Large concentration gradients are in fact generated because fluid line elements are stretched, on average, by turbulence.[10]

As discussed in more detail in Sec. II, the standard phenomenology[3-8] of passive scalars advected by turbulence envisions two simultaneous cascades. Forcing Eq. (1.4) at long wavelengths sets up the usual Kolmogorov cascade, with an energy spectrum $E(k)\sim k^{-5/3}$. The velocity field then carries concentration fluctuations down to the Kolmogorov microscale, $l_d \sim (\nu^3/\epsilon)^{1/4}$, where ϵ is the rate at which kinetic energy is injected. This concentration cascade also has the Kolmogorov exponent, $C(k)\sim k^{-5/3}$, which is plausible since the $(\vec{v}\cdot\vec{\nabla})c$ term in Eq. (1.3) implies a nonlinear time scale similar to that governing the kinetic turbulence itself. Here, $E(k)$ and $C(k)$ are proportional to the Fourier-transformed velocity and concentration correlations, respectively. Integration over all magnitudes of the scalar wave number k gives the total kinetic energy $E_{\rm tot}$ and the corresponding quantity for concentration fluctuations $C_{\rm tot}$.

Velocity fluctuations are dissipated by viscosity at scales shorter than l_d. At large Prandtl numbers $P(P=\nu/D)$, which are of order 10^3 in typical liquid mixtures, there exists a "viscous-convective" range of wave numbers greater than l_d^{-1} for which diffusion remains unimportant.[3-8] The concentration cascade continues in this regime with spectrum $C(k)\sim k^{-1}$ down to a scale $l_d' \sim l_d/\sqrt{P}$, where diffusion becomes important. If there is no mechanism for injecting concentration fluctuations into Eq. (1.3), these two cascades rapidly produce a state with $\psi(\vec{r},t)\equiv 0$.

The *equilibrium* dynamics of binary mixtures at approximately 50-50 concentrations ("active" binary mixtures), have been studied quite extensively.[11-14] The hydrodynamics of real binary mixtures involves an extra conserved density, in addition to the five conserved variables entering ordinary liquid hydrodynamics.[15] It is convenient to take this quantity to be proportional to the difference in the mass densities $\rho_A(\vec{r},t)$ and $\rho_B(\vec{r},t)$ of the two species involved,

$$\psi(\vec{r},t) \equiv [\rho_A(\vec{r},t) - \rho_B(\vec{r},t)]/\rho_0 , \tag{1.7}$$

where ρ_0 is the mean mass density. If the velocities involved in binary mixture turbulence are much less than the sound velocity, we can decouple the two sound modes by imposing incompressibility. For the special case of a *symmetric* binary mixture at 50-50 concentrations, thermal fluctuations do not appear in the concentration diffusion mode, and $\psi(\vec{r},t)$ decouples from thermal diffusion.[14] The equations of motion for the mean velocity $\vec{v}(\vec{r},t)$ and $\psi(\vec{r},t)$ then read[13,14]

$$\partial_t\psi + (\vec{v}\cdot\vec{\nabla})\psi = D\nabla^2\psi , \tag{1.8}$$

$$\partial_t\vec{v} + (\vec{v}\cdot\vec{\nabla})\vec{v} = -\frac{1}{\rho_0}\vec{\nabla}p' - \alpha\vec{\nabla}\psi\nabla^2\psi + \nu\nabla^2\vec{v} + \vec{f} , \tag{1.9a}$$

$$\vec{\nabla}\cdot\vec{v} = 0 . \tag{1.9b}$$

Several terms involving ψ have been absorbed into an effective pressure p'. These equations are identical to those for a passive scalar, except for the term involving concentration gradients in (1.9a). Its coefficient α has the dimensions of a transport coefficient squared; in Appendix A, we argue that $\sqrt{\alpha}$ is of the order of a typical fluid viscosity.

This term represents a force of the form $\mu_{AB}\vec{\nabla}\psi$, where $\mu_{AB} = -\alpha\nabla^2\psi$ is a local chemical potential

difference between the A and B components of the mixture. The dependence of μ_{AB} on ψ itself has been absorbed into the redefinition of the pressure. This thermodynamic force leads to fluid motion in response to inhomogeneities in ψ. In the presence of concentration gradients, it tends to reduce the area of surfaces of constant concentration. In this sense, the α term acts like a dynamic analog of surface tension.

The term in (1.9a) allowing concentration gradients to generate velocity fluctuations is known to be important near the critical point in Fig. 1. Together with the convective part of (1.8), it causes the equilibrium concentration diffusivity to vanish at T_c,[11-14] and leads to a weaker singularity in the shear viscosity.[13] In this sense, one can always work at high Prandtl number in mixtures by moving sufficiently close to T_c. The α term may also be significant in turbulent binary mixtures because of the violent growth of concentration gradients. When a diffusion is unimportant, a gradient of (1.8) leads to

$$D_t(\partial_i\psi) \equiv (\partial_t + \vec{v}\cdot\vec{\nabla})\partial_i\psi = (\partial_i v_j)\partial_j\psi , \tag{1.10}$$

where the summation convention has been employed. Thus, concentration gradients in fluid elements moving along a flowline increase at a rate determined by a strain rate matrix $\partial_i v_j$ with the dimensions of vorticity $\vec{\omega} = \vec{\nabla}\times\vec{v}$. But it is known that fluctuations in $\vec{\omega}(\vec{r}, t)$ grow explosively in three-dimensional turbulence, to a size limited only by viscosity.[1,16] One might expect vorticity fluctuations to drive a rapid growth of concentration gradients as well, via (1.10). If concentration gradients in binary mixtures are not dissipated before they become large, they will act back on the turbulent velocity field via the coupling in (1.9a).

C. Results and outline

Equations (1.8) and (1.9) for symmetric binary mixtures have some structural similarity to those describing magnetohydrodynamics (MHD), provided we identify the concentration difference $\psi(\vec{r}, t)$ with the magnetic vector potential.[17] MHD turbulence has been extensively studied, using both Kolmogorov-type scaling ideas[18] and phenomenological closures of the dynamical equations.[19] Turbulence in symmetric binary mixtures is perhaps most similar to *two-dimensional* MHD turbulence,[20] where the "helicity effect"[21] is absent, and where the vector potential is a scalar. Much of this MHD phenomenology can be adapted to symmetric binary mixtures.

In the absence of dissipation, there are two quadratic conserved quantities associated with symmetric binary mixtures. In addition to the squared integral of the concentration fluctuations, the quantity

$$E_{\rm tot} = \tfrac{1}{2}\int d^3r[\,|\vec{v}(\vec{r}, t)|^2 + \alpha\,|\vec{\nabla}\psi(\vec{r}, t)|^2] \tag{1.11}$$

is conserved. When concentration fluctuations are absent, one expects the standard Kolmogorov cascade of kinetic energy. More generally, however, there are peculiar wavelike excitations (similar to internal waves[22]) which transfer kinetic energy to concentration gradients and back. Under the appropriate conditions, an ultraviolet cascade in these quantities arises with inertial range spectra,[23]

$$E_v(k) \sim k^{-3/2}, \quad C(k) \sim k^{-7/2} . \tag{1.12}$$

Here, $E_v(k)$ is related to correlations in the velocity

$$E_v(k) \equiv 2\pi k^2 \int d^3r\, e^{i\vec{k}\cdot\vec{r}} \langle \vec{v}(\vec{r}, t)\cdot\vec{v}(\vec{0}, t)\rangle , \tag{1.13}$$

while

$$C(k) \equiv 2\pi k^2 \int d^3r\, e^{i\vec{k}\cdot\vec{r}} \langle \psi(\vec{r}, t)\psi(\vec{0}, t)\rangle . \tag{1.14}$$

The concentration waves, which propagate at a rate determined by the large-scale concentration gradients, are analogous to Alfvén waves in MHD. In contrast to MHD, however, the waves are overdamped in binary mixtures, and the cascades (1.12) are probably not realized in practice. Overdamped waves can, however, alter the far dissipation range, where $C(k) \sim k^{-1}$ in passive mixtures (see Sec. V).

We have studied wave effects, using a phenomenological closure of the dynamical equations, at several values of the coupling α. For large α, the waves cause concentration fluctuations to hang up, and persist for several hundred eddy turnover times. A very similar effect was uncovered by Pouquet[20] in two-dimensional MHD. Although α is too small to cause persistent concentration fluctuations at scales greater than ld in real mixtures, the effect is quite interesting; a simple explanation is provided in Sec. IV.

Studies of absolute equilibrium solutions of the system (1.8) and (1.9) allow one to predict the direction of cascades. In this way, we find a possible *infrared* cascade of concentration fluctuations to *large* length scales, with spectrum

$$C(k) \sim k^{-7/3} . \tag{1.15}$$

Such a cascade must be sustained by injection of concentration fluctuations at some intermediate wave vector. Its possible relevance to spinodal

decomposition in the two-phase region of Fig. 1 is discussed in Sec. VI.

Throughout this paper, we neglect effects due to the "intermittency" or spottiness of real turbulence.[1] Corrections to the 1941 Kolmogorov phenomenology and closure results due to intermittency often turn out to be small. Nevertheless, it would be interesting to determine how intermittency affects the results presented here.

In Sec. II, we discuss conservation laws and absolute equilibria for the symmetric binary mixture. Standard turbulence phenomenology is applied to "active" mixtures and contrasted with "passive" mixtures in Sec. III. The passive scalar phenomenology is illustrated with a simple shell model, similar to those used in studies of Navier-Stokes turbulence.[27] The eddy-damped quasinormal Markovian (EDQNM) closure is applied to the model equations in Sec. IV, where numerical results are presented. In Sec. V, we show how overdamped waves modify the viscous-convective range. Section VI dwells briefly on the relevance of our work to phase-separating binary mixtures. A more general model of turbulent binary mixtures is discussed in Appendix A. Detailed calculations relevant to the eddy-damped quasinormal Markovian closure are contained in Appendices B-E.

II. CONSERVATION LAWS AND ABSOLUTE EQUILIBRIA

Although turbulence has little direct connection with equilibrium statistical mechanics, studies of conservation laws and the associated canonical probability distribution functions have proven quite useful in uncovering trends in turbulent systems.[24,25,26] As can easily be checked from Eqs. (1.8) and (1.9), the only quadratic constants of the motion for zero dissipation and forcing are

$$C_{\rm tot} = \tfrac{1}{2}\int d^3r\, \psi^2(\vec{r},t) \tag{2.1}$$

and

$$E_{\rm tot} = E_v + E_G\,, \tag{2.2}$$

where the kinetic energy is

$$E_v = \tfrac{1}{2}\int d^3r\, |\vec{v}(\vec{r},t)|^2 \tag{2.3a}$$

and the gradient energy is

$$E_G = \tfrac{1}{2}\alpha\int d^3r\, |\vec{\nabla}\psi(\vec{r},t)|^2\,. \tag{2.3b}$$

With periodic boundary conditions, and in terms of the Fourier transforms

$$\vec{v}_{\vec{k}}(t) \equiv \int d^3r\, e^{i\vec{k}\cdot\vec{r}}\vec{v}(\vec{r},t)\,, \tag{2.4a}$$

$$\psi_{\vec{k}}(t) \equiv \int d^3r\, e^{i\vec{k}\cdot\vec{r}}\psi(\vec{r},t)\,, \tag{2.4b}$$

the (unnormalized) canonical distribution function associated with these conserved quantities is

$$\mathcal{P}(\{\vec{v}_{\vec{k}}\},\{\psi_{\vec{k}}\}) \propto \exp\Big(-\tfrac{1}{2}\sum_{\vec{k}}\,[A(|\vec{v}_{\vec{k}}|^2 + \alpha k^2|\psi_{\vec{k}}|^2) + B|\psi_{\vec{k}}|^2]\Big)\,, \tag{2.5a}$$

with

$$\vec{k}\cdot\vec{v}_{\vec{k}} = 0\,. \tag{2.5b}$$

It is easily seen that, neglecting dissipation and forcing, the distribution (2.5) is a steady-state solution of the Fokker-Planck equation associated with (1.8) and (1.9). Since forcing acts only at large length scales, and dissipation at small ones, we expect that turbulent intermediate or "inertial" scales will initially evolve towards (2.5). If it were actually possible to reach an equilibrium described by (2.5), we would have,

$$\langle |\vec{v}_{\vec{k}}|^2\rangle = 1/A\,, \tag{2.6a}$$

$$\langle |\psi_{\vec{k}}|^2\rangle = 1/(B+\alpha A k^2)\,. \tag{2.6b}$$

When $\alpha = 0$, corresponding to absolute equilibrium of a *passive* scalar, $\langle |v_k|^2\rangle$ and $\langle |\psi_k|^2\rangle$ are independent of wave number. Both A and B must be positive, and it follows that

$$E_v(k) \sim k^2, \quad C(k) \sim k^2\,. \tag{2.7}$$

Imposing an ultraviolet cutoff $k = k_{\rm max}$ to obtain finite a total energy and concentration, we see that $E_v(k)$ and $C(k)$ tend to be concentrated at large wave vectors. This ultraviolet pileup suggests the usual cascades of energy and passive scalar concentrations proposed in modern turbulence theories.

A different kind of absolute equilibrium is possible for symmetric binary mixtures with $\alpha \neq 0$. One can then have B negative, provided we require that excitations exceed a certain minimum wave number,

$$k_{\rm min} > (|B|/\alpha A)^{1/2}\,, \tag{2.8}$$

which can be very small for appropriately chosen B and A. The anomalous steady state which results (see Fig. 2) has concentration fluctuations piling up near $k_{\rm min}$, suggesting a possible *infrared* cascade of concentration fluctuations toward small wave numbers. To sustain such a cascade, one must presumably inject concentration at wave vectors $k \gg k_{\rm min}$. In Sec. VI, we show that an infrared cascade of concentration fluctuations does indeed occur for symmetric binary mixtures within the EDQNM closure. Pouquet has observed a similar cascade of vector potential fluctuations in two-dimensional MHD.[20]

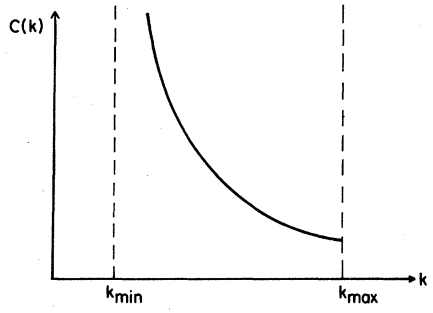

FIG. 2. The absolute equilibrium concentration spectrum $C(k)$ vs wave number for B negative. Fluctuations pile up against k_{min}, suggesting a tendency toward an inverse cascade.

Conservation laws and absolute equilibria for a more realistic model of binary mixtures are discussed in Appendix A. Two scalar fields, $\psi_1(\vec{r}, t)$ and $\psi_2(\vec{r}, t)$, representing concentration and temperature fluctuations, are convected by and allowed to react back on the velocity field. In addition to the squared integrals of ψ_1 and ψ_2, there is a quadratic conserved quantity of the form

$$E_{tot} = \tfrac{1}{2}\int d^3r(|\vec{v}|^2 + \alpha|\vec{\nabla}\psi_1|^2 + \beta|\vec{\nabla}\psi_2|^2). \quad (2.9)$$

The corresponding absolute equilibria suggest possible infrared cascades for both concentration and temperature fluctuations.

III. TURBULENCE PHENOMENOLOGY

In this section, we contrast phenomenological ideas about turbulent convection of passive scalars with the concepts necessary to describe turbulent binary mixtures. The passive scalar phenomenology will be illustrated with a simple shell model. The model displays the turbulent enhancement of the diffusivity, and exemplifies the more complicated closures of Sec. IV.

A. Shell model for passive scalars

Our aim is to construct simple, tractable caricatures of the passive scalar equations (1.3) and (1.4). The Navier-Stokes turbulence described by (1.4) has been extensively studied by this technique.[27] Let us denote by ϵ the rate of energy injection provided by the random force, and call k_{min} the wave number at which the forcing spectrum peaks. Fourier space is discretized into shells about the origin, containing the wave vector

$$k_n = k_{min} b^n . \quad (3.1)$$

Here b is a discretization parameter which exceeds unity. The basic dynamical variable is v_n^2, i.e., twice the kinetic energy contained in the nth shell,

$$v_n^2 = 4\pi\int_{k_n/\sqrt{b}}^{k_n\sqrt{b}} k^2\langle|\vec{v}_{\vec{k}}|^2\rangle\, dk = 2\int_{k_n/\sqrt{b}}^{k_n\sqrt{b}} E(k)dk . \quad (3.2)$$

In a similar way, we define a concentration variable ψ_n associated with the nth shell,

$$\psi_n^2 = 4\pi\int_{k_n/\sqrt{b}}^{k_n\sqrt{b}} k^2\langle|\psi_{\vec{k}}|^2\rangle\, dk = 2\int_{k_n/\sqrt{b}}^{k_n\sqrt{b}} C(k)dk . \quad (3.3)$$

A shell model is designed to mimic the structure of (1.3) and (1.4), preserve the conservation laws, and implement the physical idea of Kolmogorov that the important transfer of conserved quantities to small scales occurs between neighboring shells in $\vec{k}$ space. The simplest equations satisfying these requirements are

$$\frac{dv_n}{dt} = -\nu k_n^2 v_n + k_n(v_{n-1}^2 - bv_n v_{n+1}), \quad (3.4)$$

$$\frac{d\psi_n}{dt} = -Dk_n^2\psi_n + a'k_n(v_{n-1}\psi_{n-1} - bv_n\psi_{n+1}), \quad (3.5)$$

where a' is a positive constant, and $n \geq 1$. We imagine that v_0 is prescribed by the forcing

$$\frac{dv_0^2}{dt} = -\nu k_0^2 v_0^2 - bk_n v_0^2 v_1 + \epsilon \quad (3.6)$$

and set $\psi_0 \equiv 0$. It is straightforward to check that, with $\nu = D = \epsilon = 0$, the conservation laws are satisfied:

$$\frac{d}{dt}\left(\sum_n v_n^2\right) = \frac{d}{dt}\left(\sum_n \psi_n^2\right) = 0 . \quad (3.7)$$

Equation (3.4) was first studied by Desnyansky and Novikov.[27] It admits a steady-state solution of the form

$$v_n \approx \epsilon^{1/3} k_n^{-1/3} \quad (3.8)$$

for k_n in the inertial range

$$k_{min} \ll k_n \ll k_d . \quad (3.9)$$

The dissipation range wave vector k_d is

$$k_d \sim (\epsilon/\nu^3)^{1/4} \quad (3.10)$$

and, as can be seen from (3.2),

$$E(k_n) \sim v_n^2/k_n \sim k_n^{-5/3} . \quad (3.11)$$

One drawback of these shell models is that they do not admit the absolute equilibrium solutions discussed in Sec. II. Another deficiency is that the form of the steady state in the far dissipation range ($k_n \gg k_d$) depends on the discretization parameter b. Generalizing the analysis of Bell and Nelkin,[27] we find

$$E(k_n) \sim \exp(-\text{const} \times k_n^{\ln 2/\ln b}). \quad (3.12)$$

In particular, one cannot get a sensible dissipation range in the limit $b \to 1$. The partial differential equation one obtains in this way has been studied by Kovasznay[28] and Leith.[29]

To solve the passive scalar Eq. (3.5), we assume a steady-state velocity cascade has been established, and insert (3.8) to obtain (with $a' = ab^{-1/3}$)

$$\left(\frac{d}{dt} + Dk_n^2\right)\psi_n = a\epsilon^{1/3}k_n^{2/3}(\psi_{n-1} - b^{2/3}\psi_{n+1}). \quad (3.13)$$

Note that the right-hand side of (3.13) vanishes when ψ_n exhibits the Kolmogorov-type spectrum

$$\psi_n \sim k_n^{-1/3}, \quad (3.14a)$$

corresponding to[3-8]

$$C(k_n) \sim \psi_n^2/k_n \sim k_n^{-5/3}. \quad (3.14b)$$

The time dependence of Eq. (3.13) can be obtained explicitly in the limit $b \to 1$, which is well behaved in this case. Upon defining

$$g(k_n, t) \equiv k_n^{1/3}\psi_n(t) \quad (3.15)$$

and setting $b = e^{\delta}$, with $\delta \ll 1$, we obtain

$$\left(\frac{\partial}{\partial t} + Dk^2\right)g(k,t) = -2\bar{a}\epsilon^{1/3}k^{5/3}\frac{\partial g(k,t)}{\partial k}. \quad (3.16)$$

To obtain a finite result, we have assumed that a depends on b in such a way that

$$\bar{a} = \lim_{b \to 1}[a(b)\ln b] \quad (3.17)$$

exists.

The partial differential equation (3.16) is readily solved by the method of characteristics. The characteristics are a set of functions $k(t)$ parametrized by $k(t=0) = k_0$, namely,

$$k(t) = (k_0^{-2/3} - \tfrac{4}{3}\bar{a}\epsilon^{1/3}t)^{-3/2}. \quad (3.18)$$

Along these special lines, $g(k,t)$ obeys a simple ordinary differential equation

$$\frac{d}{dt}g(k(t),t) = -Dk^2(t)g(k(t),t). \quad (3.19)$$

The problem of the time evolution of $\psi_n(t)$ is now completely solved. Perhaps the most striking feature is that the characteristics bend over and reach infinite wave vectors in a finite time set by the convective nonlinearity in (3.13):

$$t_{\text{conv}}(k_0) \sim k_0^{-2/3}\epsilon^{-1/3}. \quad (3.20)$$

Initial data specified for $k \geq k_{\min}$ in Fig. 3 is swept away in a time of order $k_{\min}^{-2/3}\epsilon^{-1/3}$. If concentration is constantly injected along the vertical line at $k_{\min}$, a universal steady state, independent of the initial data, is established above the characteristic with $k_0 = k_{\min}$. Since $t_{\text{conv}}(k_{\min})$ is much less than the diffusion time at $k_{\min}$ for large ϵ and small D,

$$t_{\text{conv}}(k_{\min}) \ll t_{\text{diff}} \equiv 1/Dk_{\min}^2, \quad (3.21)$$

there is an enormous increase in the efficiency of mixing. Plots of $C(k,t)$ obtained from (3.18) and (3.19) with initial data concentrated near $k_{\min}$ are displayed in Fig. 4. The Kolmogorov spectrum (3.14b) is established quickly, and then decays rapidly to zero in a self-similar fashion.

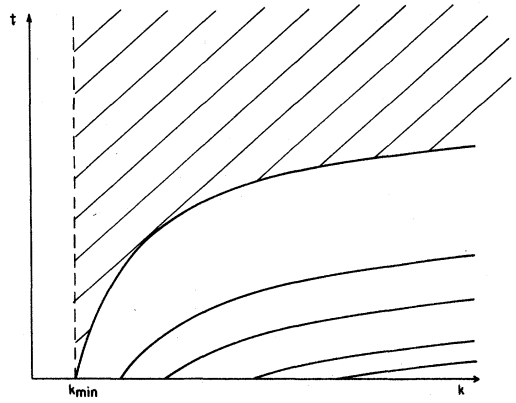

FIG. 3. Characteristic curves $k_c(t)$ for Eq. (3.16). The concentration fluctuations in the shaded region are independent of the initial conditions and depend only on the boundary conditions at $k_{\min}$. The rapid growth with increasing time of the length of the line t = constant joining two characteristics reflects the violent turbulent stretching of concentration gradients.

As mentioned in the Introduction, one has Prandtl numbers $P = \nu/D$ much larger than unity in typical mixtures. The physics of passive scalars then changes in the viscous-convective range of wave vectors exceeding k_d.[3-8] Since there are no appreciable velocity fluctuations in this range, the smallest eddy turnover time effective in transferring concentration between shells with $k_n > k_d$ is just the time appropriate to k_d itself. It is a simple exercise to show from (3.4) that this time is

$$t_d = \epsilon^{-1/3}k_d^{-2/3} = 1/\nu k_d^2. \quad (3.22)$$

One imagines that transfer of concentration between neighboring shells is controlled by a random strain rate with a characteristic time (3.22).[5] A simple modification of the shell model (3.13) which incorporates these physical ideas is

$$\left(\frac{d}{dt} + Dk_n^2\right)\psi_n(t) = a\left(\frac{\epsilon}{\nu}\right)^{1/2}(\psi_{n-1} - \psi_n). \quad (3.23)$$

Passing to a partial differential equation as before, we find a steady state with

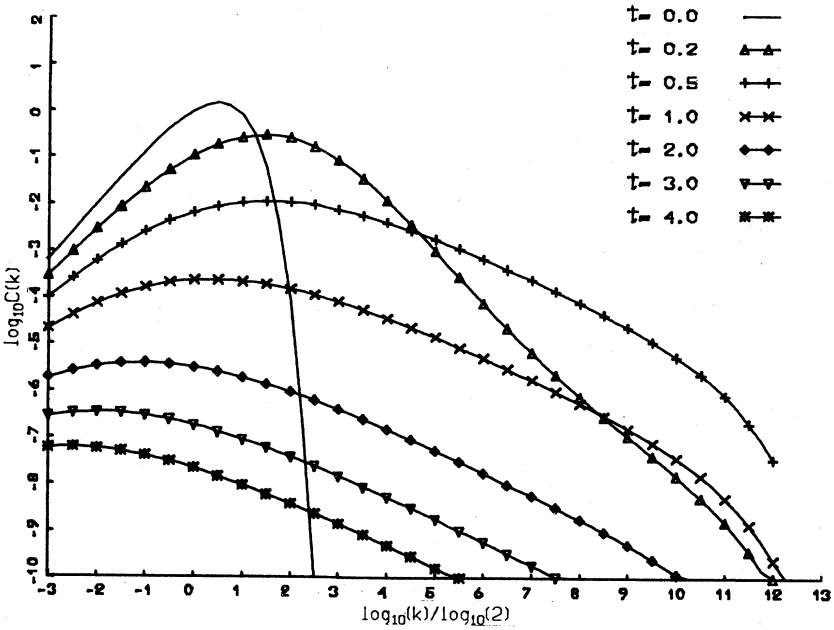

FIG. 4. Time evolution of the concentration spectrum with $P \ll 1$ obtained from (3.16). The driving velocity field satisfies $E_k \sim k^{-5/3}$ for all wave numbers displayed. The time is measured in units of $t_{\mathrm{conv}}(k_0)$.

$$C(k) \approx C(k_d)(k_d/k)\exp(-k^2/k_d^2 \bar{a} P). \tag{3.24}$$

This result was first obtained by Batchelor.[5]

The characteristics of the partial differential equation associated with (3.23) when $b \to 1$ are

$$k(t) = k_0 e^{\bar{a}\sqrt{\epsilon/\nu}\, t}. \tag{3.25}$$

It now takes an infinite time for information to propagate to infinite wave vectors. For finite diffusivities D, the concentration is finally dissipated at a wave vector

$$k_d' = k_d \sqrt{\nu/D}. \tag{3.26}$$

B. Symmetric binary mixture phenomenology

If the term coupling concentration gradients back into the velocity field in (1.9a) is negligible the passive scalar phenomenology is of course applicable to symmetric binary mixtures. We have already seen in Sec. II, however, that this term suggests an inverse cascade of concentration fluctuations not present for passive mixtures. This coupling also leads to transverse waves in the presence of concentration gradients. Although these waves resemble "internal waves" in stratified fluids,[22] the restoring force is not gravity, but a surface-tension-like effect.

The concentration waves can be studied by imposing a uniform concentration gradient B_0, and linearizing about the state

$$(\vec{\nabla}\psi)_0 \equiv \vec{B}_0, \quad \vec{v}_0 = 0. \tag{3.27}$$

Carrying out this linearization in the absence of forcing, we find

$$\partial_t \psi \approx -\vec{v}\cdot\vec{B}_0 + D\nabla^2\psi, \tag{3.28a}$$

$$\partial_t \vec{v} \approx -\alpha \vec{B}_0 (\vec{\nabla}\cdot\vec{b}) + \nu\nabla^2\vec{v}, \tag{3.28b}$$

where $\vec{b}(\vec{r}, t)$ represents a small deviation of concentration gradients from uniformity,

$$\vec{\nabla}\psi(\vec{r}, t) \equiv \vec{B}_0 + \vec{b}(\vec{r}, t). \tag{3.29}$$

The α term (3.28b) tends to even out inhomogeneities in the concentration gradients; i.e., it tends to produce parallel straight lines of constant concentration. In this sense, it is like a surface tension. Taking care to enforce incompressibility, it is straightforward to find wavelike solutions of (3.28) where $\vec{b}(\vec{r}, t)$ and $\vec{v}(\vec{r}, t)$ vary like $e^{i\vec{k}_0\cdot\vec{r} - i\omega(k)t}$. In the limit of small damping, the dispersion relation is

$$\omega(k) = \pm\sqrt{\alpha}\,|\vec{k}\times\vec{B}_0| - \tfrac{1}{2}i(D+\nu)k^2. \tag{3.30}$$

As can be seen from Fig. 5, the velocity is directed along $\vec{B}_0$, while $\vec{b}(\vec{r}, t)$ varies perpendicular to this direction.

Concentration waves in symmetric binary mixtures resemble the Alfvén waves of magnetohydrodynamics[30]; although Alfvén waves propagate along the magnetic field lines, concentration waves propagate perpendicular to the direction singled

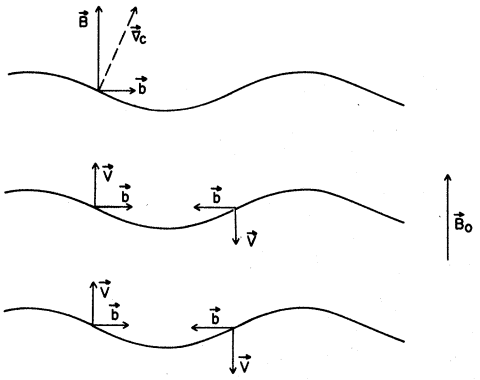

FIG. 5. Geometry of the wave propagation. The lines are contours of constant concentration.

out by $\vec{B}_0$. In Appendix A, we argue that α is of order of shear viscosity squared in real fluids. Consequently, the concentration waves will be heavily damped unless B_0 is extremely large.

The relevance of Alfvén waves to MHD turbulence has been discussed by Kraichnan.[18] Random, large-scale magnetic fields lead to a new inertial range time scale, given by the period of the corresponding Alfvén waves. At sufficiently high wave numbers this time is shorter than the one entering the Kolmogorov phenomenology. A new kind of turbulence results, dominated by "nonlocal" interactions between small and large wave vectors in Fourier space. Kraichnan argued that the Alfvén waves would bring the magnetic and kinetic energies into equipartition. Largely on dimensional grounds, he suggested that the velocity spectrum would be

$$E(k) \sim (\epsilon B_0)^{1/2} k^{-3/2}, \tag{3.31}$$

where B_0 is the root-mean-square fluctuation in the large-scale magnetic field. A similar result holds for the magnetic field spectum.

Kraichnan's arguments carry over, in principle, to symmetric binary mixtures, implying equipartition of the two energies in (1.11) and $k^{-3/2}$ spectra. Because α is so small, however, concentration waves probably never become important before the dissipation range is reached. The most important effect of the concentration waves is to shorten the viscous-convective cascade referred to in the previous subsection. Because concentration gradients can be transformed in velocity fluctuations and then dissipated, no appreciable concentration fluctuations will exist beyond a cutoff wave vector appreciably smaller than the passive scalar cutoff k_d'. As discussed in Sec. V, the k^{-1} spectrum proposed by Batchelor[5] for passive mixtures is truncated prematurely. The effect of waves on binary mixtures with large α is studied by a closure technique in Sec. IV.

There remains the possibility, under certain circumstances, of an inverse cascade of concentration fluctuations. If concentration fluctuations are injected at a rate ϵ_ψ, dimensional analysis suggests that the form of the concentration spectrum cascading toward large length scales is

$$C(k) = \epsilon_\psi^{2/3} k^{-7/3}, \tag{3.32}$$

in analogy to an inverse cascade of magnetic vector potential in two dimensions.[20] The relevance to this cascade to spinodal decomposition is discussed in Sec. VI.

IV. EDDY-DAMPED QUASINORMAL MARKOVIAN CLOSURE

A. The EDQNM equations

There has been, in the last decade, remarkable progress in the construction of closure equations[1] for turbulence which (1) incorporate the Kolmogorov phenomenology in a more precise mathematical setting and (2) determine the time evolution of spectra from arbitrary initial conditions. In this paper we use the EDQNM closure used previously for the study of the Navier-Stokes[31,32] and MHD turbulence.[19,20] As discussed in Ref. 1, this closure links the fourth-order cumulants (C_4) phenomenologically to the third-order ones (C_3) by means of an eddy relaxation operator μ,

$$C_4 \sim \mu C_3. \tag{4.1}$$

The EDQNM closure can be regarded as a more elaborate version of the simple shell-model equations of Sec. III A. The closure preserves the conservation laws and absolute equilibria of the primitive equations.[33] Simple physical ideas governing cascades are incorporated into "triad relaxation times." The closure can then be used to predict the direction of cascades and the time evolution of spectra. In this sense, closure such as the one used here represent a kind of crude "mean field theory" of turbulence. The phenomenological spectral exponents are built in.

When Eq. (4.1) is used to close the hierarchy of cumulant equations derived from (1.8) and (1.9), we obtain equations for the spectra of the kinetic energy and the concentration fluctuations. Assuming homogeneity and statistical isotropy of our system, these equations have the form

$$(\partial_t + 2Dk^2)C(k) = T_c(k), \tag{4.2}$$

$$(\partial_t + 2\nu k^2)E_v(k) = T_v(k) + F(k), \tag{4.3}$$

where $F(k)$ is related to the force (see below), and $T_c(k)$ and $T_v(k)$ are "transfer integrals" discussed below. The transfer integrals for symmetric binary mixtures in d dimensions are worked out in Appendix B. Specializing to $d=3$, we find

$$T_c(k)=2\int_{\Delta_k}\int dp\,dq\left(\frac{\sin\beta}{k}\right)^2\frac{kq}{p}\,\theta^{(1)}_{kpq}\left\{\tfrac{1}{2}E_v(p)[k^2C(q)-q^2C(k)]-\alpha(k^2-q^2)p^2C(k)C(q)\right\} \tag{4.4}$$

and

$$T_v(k)=\int_{\Delta_k}\int dp\,dq\,\frac{1}{kpq}\left[\theta^{(2)}_{kpq}b_{kpq}E_v(q)[k^2E_v(p)-p^2E_v(k)]\right.$$
$$\left.+\,\theta^{(3)}_{kpq}\left(\frac{\sin\beta}{k}\right)^2p^2q^2(p^2-q^2)[\alpha^2(p^2-q^2)k^2C(p)C(q)-\alpha p^2C(q)E_v(k)]\right]. \tag{4.5}$$

The double integral is restricted by momentum conservation to wave-vector magnitudes p and q such that $\vec{k}$, $\vec{p}$, and $\vec{q}$ form a triangle. We have averaged over the random force (or, equivalently, over different turbulent realizations), and $F(k)$ is the power spectrum of the forcing, assumed to be Gaussian white noise for convenience. Turbulence at small scales should be independent of the details of the large-scale forcing. In (4.5), b_{kpq} is the usual geometrical coefficient[31,32]

$$b_{kpq}=\frac{1}{2k^2}\left(\frac{\sin\beta}{k}\right)^2[k^2p^2+(p^2-q^2)(k^2-q^2)], \tag{4.6}$$

where β is the angle opposite to wave vector k in the triangle formed by k, p, and q.

The quantities $\theta^{(i)}_{kpq}(t)$, $(i=1,2,3)$, are called the *triad relaxation times*; their choice is the main feature that differentiates alternate schemes of closure. For the particular case of the EDQNM closure they take the form[31,32]

$$\theta^{(i)}_{kpq}(t)=\frac{1-e^{-t\mu^{(i)}_{kpq}}}{\mu^{(i)}_{kpq}}, \tag{4.7}$$

where

$$\begin{aligned}\mu^{(1)}_{kpq}&=\mu^c_k+\mu^v_p+\mu^c_q,\\ \mu^{(2)}_{kpq}&=\mu^v_k+\mu^v_p+\mu^v_c,\\ \mu^{(3)}_{kpq}&=\mu^v_k+\mu^c_p+\mu^c_q,\end{aligned} \tag{4.8}$$

and

$$\mu^c_k-Dk^2=\mu^v_k-\nu k^2$$
$$=C_E\left(\int_0^k dq\,q^2E(q)\right)^{1/2}+C_w k\left(\int_0^k dq\,\alpha q^2C(q)\right)^{1/2}. \tag{4.9}$$

The terms proportional to D and ν are generated automatically in a perturbative treatment of the nonlinearities. Their presence ensures the existence of proper dissipation ranges for the spectra. The term proportional to C_E in (4.9) is the inverse eddy turnover time for the velocity field.[1] It is designed to model the characteristic time associated with convective transfer, which dominates in ordinary Navier-Stokes turbulence. The constant C_E itself can be fit to experiments on Navier-Stokes turbulence, and was determined in Ref. 32 to be $C_E\approx 0.360$. The term proportional to C_w is the inverse period of the concentration waves discussed in Sec. III B. We have only attempted to model the tendency toward equipartition when dissipation can be neglected. Although C_w is a free parameter of the closure, a simple self-consistency argument presented in Appendix D suggests we take $C_w=1$.

If one sets $C(k)\equiv 0$ in (4.4) and (4.5), we recover the closure used to study Navier-Stokes turbulence in Refs. 31 and 32. In the limit $\alpha\to 0$, we model turbulent convection of a passive scalar, which was studied via a slightly different closure in Ref. 6.

B. Conservation laws and inertial range spectra

Given the importance of conservation laws in the Kolmogorov-type phenomenological arguments for turbulent systems, it is important to check that the quantities conserved by our original equations (1.8) and (1.9) are also conserved by the spectral equations (4.2) and (4.3). One can indeed check easily the following:

(a) The closure equations are not only compatible with the conservation laws of the quantities (2.1) and (2.2), but also with detailed conservation of the same quantities by any of the interacting wave-vector triads.[24] More explicitly, if we write (4.4) and (4.5) as

$$T_{v,c}(k)\equiv\int_{\Delta_k}\int dp\,dq\;T_{v,c}(k\,|pq)$$
$$=\tfrac{1}{2}\int_{\Delta}\int dp\,dq[T_{v,c}(k\,|pq)+T_{v,c}(k\,|qp)]$$
$$\equiv\tfrac{1}{2}\int_{\Delta}\int dp\,dq\;T^{v,c}_{\rm sym}(k\,|pq), \tag{4.10}$$

detailed conservation means

$$T^c_{\rm sym}(k\,|pq) + T^c_{\rm sym}(q\,|kp) + T^c_{\rm sym}(p\,|qk) = 0 \quad (4.11)$$

and

$$[T^v_{\rm sym}(k\,|pq) + \alpha k^2 T^c_{\rm sym}(k\,|pq)] + \text{c.p.} = 0\,, \quad (4.12)$$

where c.p. represents all cyclic permutations.

Upon integration over k, (4.11) and (4.12) are equivalent to

$$\int_0^\infty dk\, T_c(k) = 0 \quad (4.13)$$

and

$$\int_0^\infty dk[T_v(k) + \alpha k^2 T_c(k)] = 0\,, \quad (4.14)$$

which in turn imply the conservation laws.

(b) The absolute equilibrium spectra (2.6) are in fact steady-state solutions of the spectral equations in the limit $D=\nu=F_k=0$, provided the spectra are bounded by some $k_{\max}$. One can prove, using the techniques of Ref. 33, that these are the only steady-state solutions in this limit.

The procedure used to extract the inertial range spectral exponents from Eqs. (4.2) to (4.5) is outlined in Appendix C. The results for different regimes are summarized in Table I. The scaling behavior of the triad relaxation time is crucial in determining the power-law exponents for the spectra. The second column of Table I contains the term of μ_k that dominates in each case. It is conventional to say that there is a cascade of some conserved quantity Q if there is a range of scales where the quantity $\Pi_Q(q)$, defined by

$$\Pi_Q(k) = -\int_0^k dq\, T_Q(q)\,, \quad (4.15)$$

is independent of k.[1] The quantity $\Pi_Q(k)$ corresponds to the rate of energy injection and dissipation entering phenomenology theories in the steady state. In this way, we associate with each inertial range some kind of a cascade, as compiled in the table.

C. Closure results for passive mixtures ($\alpha = 0$)

The closure equations (4.2)–(4.5) are too complicated to be solved analytically. Here, we present numerical results for "passive" mixtures, with α set to zero. The analysis serves as a check on the equations themselves, and complements the passive scalar phenomenology of Sec. III A. The EDQNM equations were integrated numerically using a modification of the method used, for example, by Leith.[34]

Figures 6 and 7 illustrate the time evolution of kinetic energy and concentration spectra with a large-scale, band-limited forcing. At time $t=0$, all concentration fluctuations reside in the large scales. Figure 6 shows how the usual $k^{-5/3}$ cascade in kinetic energy is established. Also shown

TABLE I. Summary of the different regimes, cascades, and spectral exponents allowed by our closure equations. Column 2 contains the dominant term of the relaxation operator μ for each regime. In the fourth and fifth columns, the cascades are listed as ultraviolet (infrared) if they evolve towards the small (large) scales.

Regime	Dominant μ_k	Spectra	$C_{\rm cascade}$	$E_{\rm cascade}$
NSE $C(k)=0$ $\alpha=0$	$\mu_k \sim \left(\int_0^\infty dq\; q^2 E(q)\right)^{1/2}$	$E(k)\sim k^{-5/3}$		UV (E_v)
Passive scalar $C(k)\neq 0$, $\alpha=0$	$\mu_k \sim \left(\int_0^k dq\; q^2 E(q)\right)^{1/2}$	$E(k)\sim k^{-5/3}$ $C(k)\sim k^{-5/3}$	UV	UV (E_v)
Viscous convective passive regime $(k \gg k_d)$, $E(k)\sim 0$	$\mu_k \sim \sqrt{\epsilon/\nu}$	$E(k)$ decaying $C(k)\sim k^{-1}$	UV	
Active mixtures $\alpha=1$	$\mu_k \sim \left(\int_0^k dq\; q^2 E(q)\right)^{1/2}$	$E(k)\sim k^{-5/3}$ $C(k)\sim k^{-5/3}$	UV	UV
	$\mu_k \sim \left(\int_0^k dq\; q^2 E(q)\right)^{1/2}$	$C(k)\sim k^{-7/3}$ $E(k)\sim k^{-1/3}$	IR	
	$\mu_k \sim \left(\int_0^k q^2 C(q) dq\right)^{1/2}$	$C(k)\sim k^{-7/2}$ $E(k)\sim k^{-3/2}$		UV (of $E_v + E_G$)

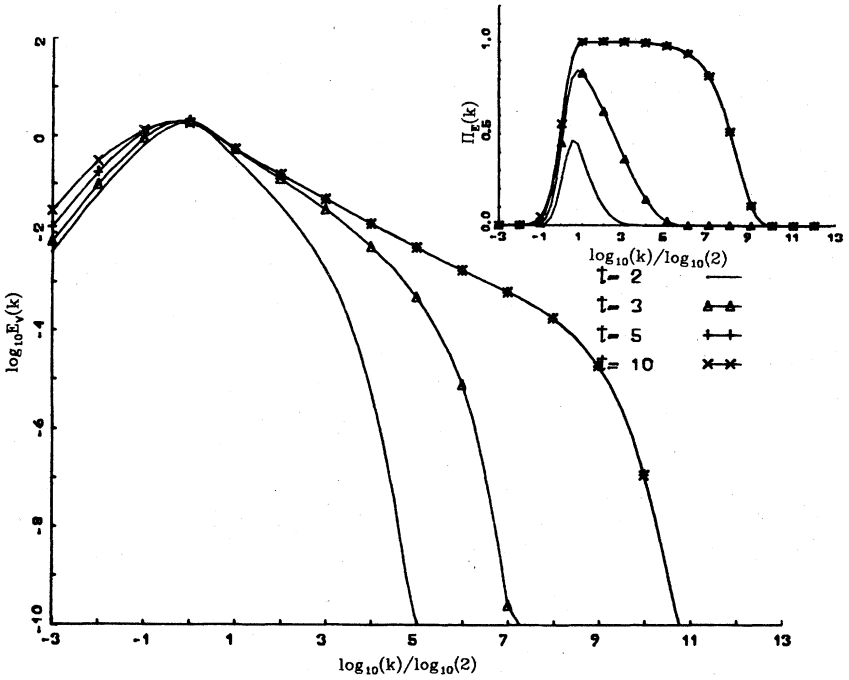

FIG. 6. Evolution of the kinetic spectrum $E_v(k)$ with time for $\alpha=0$. The units are such that $\epsilon=\int_0^\infty dk\,F(k)=1$, and $F(k)$ peaks at $k\equiv k_0=1$. The viscosity is $\nu=10^{-4}$ in these units. Time is measured in eddy-turnover times at k_0, and the initial energy was zero. The Reynolds number is $R\simeq\langle v^2\rangle^{1/2}/\nu k_0\simeq 10^4$ in the steady state. The quantity $\Pi_{E_v}(k)$ is shown in the inset.

is the kinetic dissipation rate $\Pi_{E_v}(k)$ defined by (4.15). Once the cascade of velocity fluctuations is set up, this quantity is a constant in the inertial range. Concentration fluctuations are dissipated by the Navier-Stokes turbulence in Fig. 7. After a few large eddy turnover times t_0 ($t_0\sim l_0/v_0$, where v_0 is a typical velocity at the largest scale l_0), $C(k)$ displays a time-dependent $k^{-5/3}$ cascade, and then decays rapidly to zero. The concentration dissipation rate $\Pi_c(k)$ is shown for $t=10\ t_0$ in the inset.

In Fig. 8 we have plotted the time variation of $C_{\rm tot}(t)$, together with the kinetic dissipation rate K. This latter quantity is simply related to the mean-squared vorticity when $\alpha=0$,

$$K=2\nu\int_0^\infty k^2E_v(k)dk\equiv 2\nu\Omega(t)\,. \tag{4.16}$$

Since a steady state is achieved when this quantity equals the kinetic energy injection rate ϵ, we expect $\Omega(t)$ to rise rapidly in Navier-Stokes turbulence to a value $\epsilon/2\nu$. The abrupt increase of the kinetic dissipation rate near $t=3.5t_0$ is consistent with the explosive singularity in $\Omega(t)$ found by Morf *et al.*[16] in a simulation of the Taylor-Green vortex. The rise in $\Omega(t)$ is accompanied by a sudden decay in the total concentration, which is unchanged prior to this time.

Analytic insight into this behavior can be obtained using the Markovian random-coupling model,[35] in which one simplifies closures by arbitrarily setting all triad relaxation times to a constant θ. One then finds analytically in d dimensions that, $\nu=f=0$,

$$\Omega(t)=\frac{\Omega(0)}{1-G(d-2)\Omega(0)\theta_0 t}\,, \tag{4.17}$$

where G is a dimensionality-dependent constant.[1] The simple pole in $\Omega(t)$ one finds at $t^*=1/G(d-2)\Omega(0)\theta_0$ should be compared with the behavior

$$\Omega(t)\sim|t-t^*|^{-0.8} \tag{4.18}$$

found by Morf *et al.*[16] It is easily shown that the dissipation rate of concentration fluctuations is

$$\frac{dC_{\rm tot}}{dt}=-2D\int_0^\infty k^2C(k)dk\equiv-2DE_G\,. \tag{4.19}$$

In Appendix E, we show that the Markovian random-coupling model predicts that the gradient energy $E_G(k)$ obeys

$$\frac{dE_G(t)}{dt}=G(d-1)\Omega(t)E_G(t)\,. \tag{4.20}$$

The singularity in $\Omega(t)$ means that $E_G(t)$ also diverges at t^*,

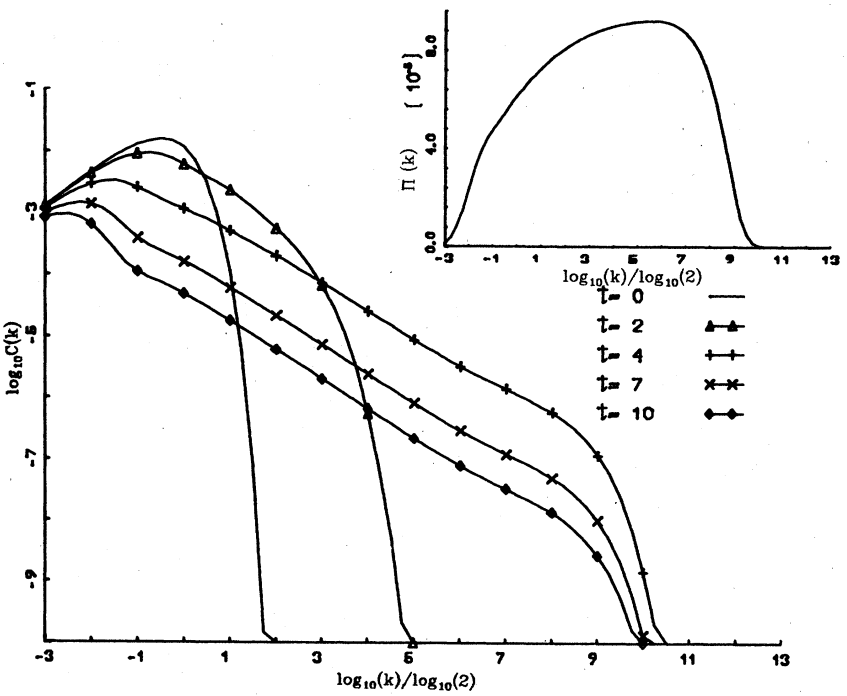

FIG. 7. Evolution of $C(k)$ for $\alpha=0$. The driving velocity field is that of Fig. 6, and the Prandtl number is $P=1$. The normalization is such that $C_{\rm tot}(t=0)=1.3\times10^{-2}$. The inset displays the plateau of $\Pi_c(k)$ at $t=10$ that manifests the cascade of the concentration fluctuations.

$$E_G(t)=\frac{E_G(0)}{[1-G(d-2)\Omega(0)t]^{(d-1)/(d-2)}}\,. \tag{4.21}$$

This explosive singularity goes over into an exponential increase in time in two dimensions, where Ω is conserved. An explosive growth of concentration gradients analogous to (4.21) is associated with the sudden decrease in $C_{\rm tot}(t)$ shown for $t\approx3.5t_0$ in Fig. 8.

The Kolmogorov phenomenology asserts that the dominant transfer of conserved quantities occurs between neighboring scales in Fourier space. In reality, nonlinear interactions occur between all triads of wave vectors $\vec{k}$, $\vec{p}$, and $\vec{q}$ such that $\vec{k}+\vec{p}+\vec{q}=0$, and not just among those forming nearly equilateral triangles. The "nonlocality" of interactions between widely separated scales in Fourier space is measured by a shape parameter

$$A=\frac{\max(k,p,q)}{\min(k,p,q)}\,. \tag{4.22}$$

As explained in Ref. 36, it is possible to carry out a systematic expansion of the transfer integrals (4.4) and (4.5) in powers of $1/A$, while keeping the conservation laws intact. Since the calculations are long and tedious, we simply summarize the results as they apply to passive scalars.

The nonlocal effects of small-scale velocity and concentration fluctuations on the large-scale concentration are represented by the long narrow triangle shown in Fig. 9(a). To leading order in A^{-1}, these small scales give a contribution to

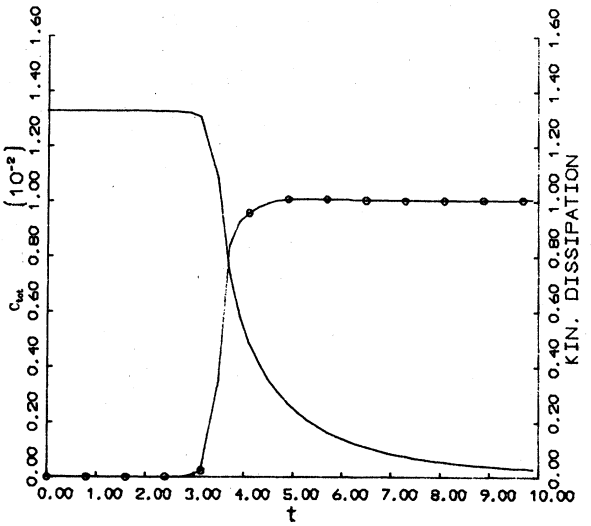

FIG. 8. Time evolution of $C_{\rm tot}(t)=\int_0^\infty dk\,C(k,t)$ (——) and the kinetic dissipation rate $\epsilon(t)=2\nu\int_0^\infty k^2E_v(k)\,dk$ (-o-o-o-) for the run displayed in Figs. 6 and 7. Note the sudden onset of the dissipation. The quantity $\epsilon(t)$ is constant in the steady state.

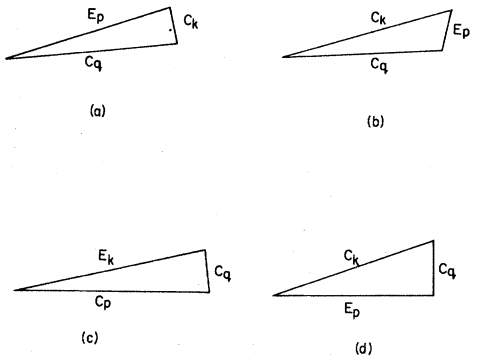

FIG. 9. Types of triads contributing to the nonlocal interactions discussed in the text. Figure (a) represents the contribution to the turbulent eddy diffusivity (4.24b). The triad of (b) dominates in the viscous convective regime. The triads (c) and (d) represent the action of the waves on the small scales.

$T_c(k)$ (with $\alpha \equiv 0$) of the form

$$[T_c(k)]_{ss} = - D_{\text{turb}}(k) k^2 C(k), \tag{4.23a}$$

where

$$D_{\text{turb}}(k) = \tfrac{4}{3} \int_k^\infty dq\, \theta^{(1)}_{kqq} E_v(q). \tag{4.23b}$$

The turbulent eddy diffusivity $D_{\text{turb}}(k)$ represents the enhanced dissipation of concentration fluctuations due to turbulence. Approximating θ_{kqq} by[1] $[E(q)q^3]^{-1/2}$ and inserting $E_v(q) \sim q^{-5/3}$, we recover the famous result first obtained by Richardson[37]:

$$D_{\text{turb}}(k) \sim (k_d/k)^{4/3}. \tag{4.24}$$

Nonlocal interactions are also important in the high Prandtl number viscous-convective range $k > k_d$ discussed in Sec. III A. The evolution of $C(k)$ in this range is controlled by the triad shown in Fig. 9(b), which couples $C(k)$ to scales larger than k_d^{-1}. As shown by Kraichnan,[6] such triads give a contribution from the large scales to $T_c(k)$,

$$[T_c(k)]_{ls} = \frac{2}{15}\left(\int_0^{k_d} dp\, \theta^{(1)}_{kpk} p^2 E_v(p)\right) \times \left(k^2 \frac{\partial^2 C(k)}{\partial k^2} - 2C(k)\right), \tag{4.25}$$

in three dimensions. This term is reminiscent of the right-hand side of the shell-model equation (3.23). Both the usual viscous-convective spectrum $C(k) \sim k^{-1}$ and absolute equilibrium $[C(k) \sim k^2]$ cause this nonlocal part of the transfer to vanish.

D. Closure results for active mixtures (α large)

We have also integrated the closure equations in the more interesting case $\alpha \neq 0$. To enhance the effects of concentration waves, we have set $\alpha \equiv 1$ (in units such that $\epsilon = 1$ and $k_0 = 1$), which is unrealistically large. By understanding the effect of waves in this limit, we can see why they are in fact unimportant in the inertial range of realistic binary mixtures. The waves do, however, play a

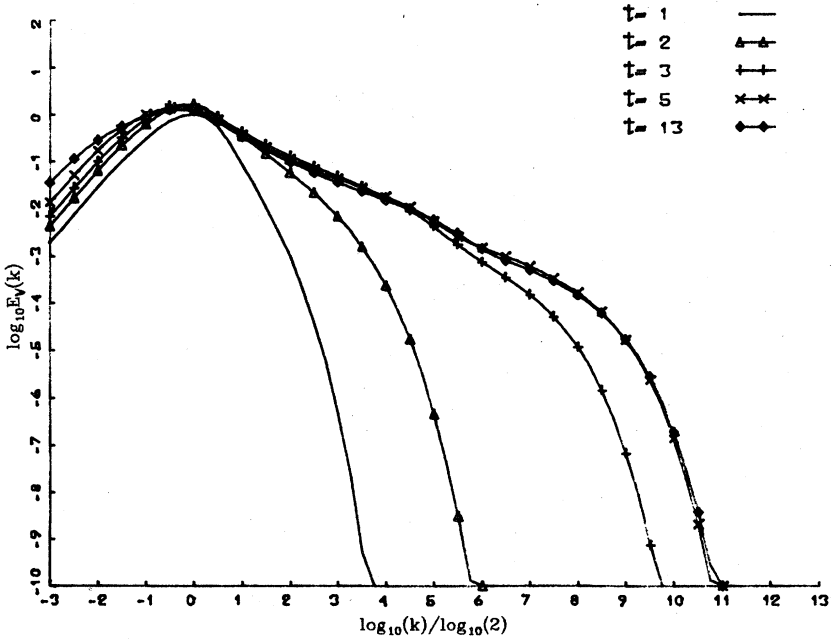

FIG. 10. Evolution of $E_v(k)$ with time for $\alpha = 1$. The units and all the other parameters are identical to those of Fig. 6.

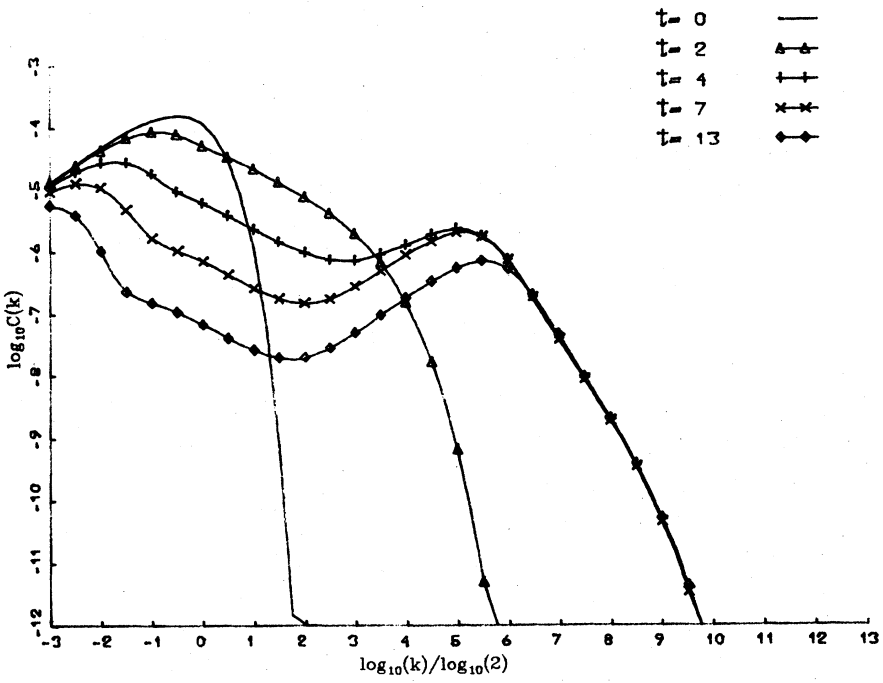

FIG. 11. Time evolution of $C(k)$ for $\alpha=1$. The driving velocity field is that of Fig. 10, and the Prandtl number is $P=1$. The initial conditions had $C_{\rm tot}(0)=10^{-4}$. The differences with Fig. 7 are due to concentration wave effects.

role in the viscous-convective range of high-Prandtl-number fluids. We have set $\nu=D$ in the large-α limit for simplicity.

In Figs. 10 and 11 we show the time evolution of $E_v(k)$ and $C(k)$ with the same forcing and initial conditions as for $\alpha=0$. The presence of two distinct regimes is most manifest in the concentration spectrum. Figure 11 shows a passive scalar spectrum at low k and gives $C(k)\sim k^{-7/2}$ at higher wave numbers. As shown in Fig. 12, there is approximate equipartition between $E_v(k)$ and $2\alpha k^2C(k)$ in this high wave-vector range, where $E_v(k)\sim k^2C(k)\sim k^{-3/2}$. The two regions of $\vec{k}$ space are separated by a wave vector k_c at which the concentration peaks up. The high-k region is evidently dominated by waves with a frequency given by Eq. (3.31),[18]

$$\omega(k)\sim[k_c^3C(k_c)]^{1/2}k\,. \tag{4.26}$$

The quantity B_0 has been replaced by the root-mean-square large-scale concentration gradient,

$$B(k_c)\equiv(\nabla\psi)_{\rm rms}\approx\left(\int_0^{k_c}k^2C(k)dk\right)^{1/2}\approx[k_c^3C(k_c)]^{1/2}\,. \tag{4.27}$$

The effects of waves can be understood more quantitatively by considering the nonlocal portions of the transfer displayed in Figs. 9(c) and 9(d).[19] Considering the effect of large scales on transfers with $k>k_c$, we find contributions

$$[T_v(k)]_{ls}=\tfrac{4}{3}\alpha\left(\int_0^{k/A}dq\,\theta_{kkq}q^2C(q)\right)k^2[2\alpha k^2C(k)-E(k)]\,, \tag{4.28a}$$

$$[T_c(k)]_{ls}=\frac{4}{3}\left(\int_0^{k/A}dq\,\theta_{kkq}q^2C(q)\right)[E(k)-2\alpha k^2C(k)]\,, \tag{4.28b}$$

where A is given by (4.23). When combined with (4.2) and (4.3), these results imply the approach to the equipartition displayed in Fig. 12. The ratio $E(k)/\alpha k^2C(k)$ tends to 2 because there are two independent (transverse) components of the velocity; the waves produce equipartition between each velocity component and the single concentration degree of freedom.

Although we have not yet done simulations at high Prandtl number, the results (for $\alpha=1$) must be qualitatively unchanged. No concentration gradients are possible for $k>k_d$ since the waves enforce equipartition beyond k_c. A nascent concentration gradient with $k>k_d$ would be converted into kinetic energy and dissipated.

A consequence of concentration waves which was unanticipated by the phenomenology of Sec. III is shown in Fig. 13. In contrast to the passive case $\alpha=0$, concentration fluctuations take an exceedingly long time to decay. The decay would be even slower if D were lowered to more realistic

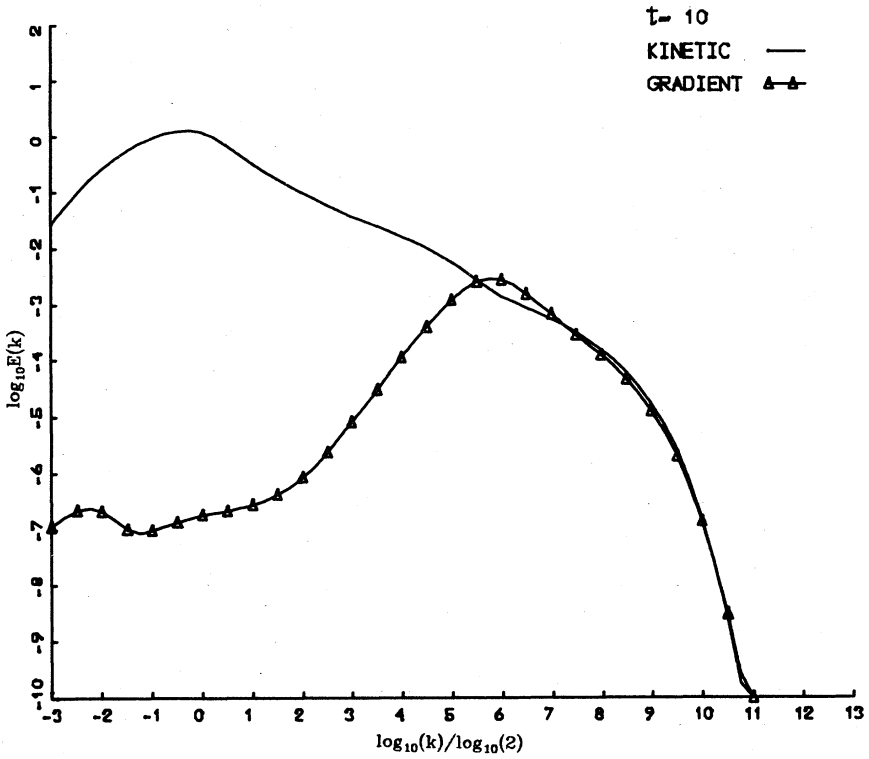

FIG. 12. A graph displaying the approximate equipartition between $E_v(k)$ (——) and $E_G(k)=2\alpha k^2 C(k)$ (-△-△-) induced by the waves. The spectra are those of Figs. 10 and 11 at $t=10$.

values. A very similar persistence of vector-potential fluctuations was observed by Pouquet in two-dimensional MHD turbulence.[20]

This slow mixing can be understood by using (4.19) to estimate the concentration dissipation rate. Using $C(k)\sim k^{-7/2}$ we find

$$\frac{dC_{\rm tot}}{dt}\approx -2D\int_{k_c}^{\infty} k^2 C(k)dk \approx -2DC(k_c)k_c^3. \quad (4.29)$$

Because of the steep concentration spectrum the integral is dominated by its lower limit. This is not the case for the more gentle $k^{-5/3}$ passive scalar spectrum. Using an estimate of the stretching of concentration gradients by the passive scalar cascade between k_0 and k_c, we find

$$C(k_c)k_c^3 \approx \left(\frac{k_c}{k_0}\right)^{4/3} C(k_0)k_0^3. \quad (4.30a)$$

Since $C_{\rm tot}\approx k_0 C(k_0)$, Eqs. (4.29) and (4.30a) imply a time scale for turbulent mixing:

$$\tau_c \approx 1/Dk_0^2(k_c/k_0)^{4/3}. \quad (4.30b)$$

We can regard this formula as an application of the Richardson formula (4.25) for the turbulent diffusivity acting on the concentration at k_0, except that k_d has been replaced by k_c. Since $k_c \ll k_d$ for large α, the turbulent enhancement of the diffusivity is significantly diminished by the concentration waves. For small D, τ_c can be quite long.

To determine the importance of this effect in real mixtures, it is crucial to estimate k_c. Wave effects should become important when their period becomes comparable to the convective nonlinear timescale (3.20), which gives

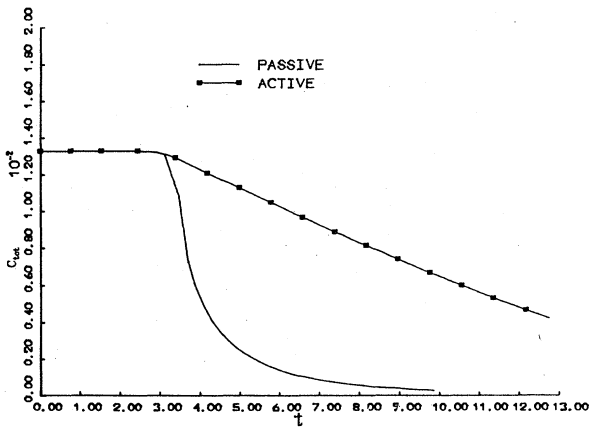

FIG. 13. Comparison of the decay of $C_{\rm tot}(t)$ for active (——) and passive (-▫-▫-) mixtures. The conditions are those of Figs. 7 and 10. ($P=1$ in both cases.)

$$k_c = \epsilon/\alpha^{3/2}[\vec{\nabla}\psi(t_c)]^3_{\rm rms}\,. \tag{4.31}$$

The root-mean-square concentration gradient appearing in (4.31) is evaluated at a time t_c such that the concentration gradients have been stretched sufficiently to sustain the waves in a quasi-steady state beyond k_c. At times $t < t_c$, one has a formula analogous to (4.27):

$$[\vec{\nabla}\psi(t)]_{\rm rms} = \left(\int_0^{k_{\max}(t)} k^2 C(k,t)\,dk\right)^{1/2}, \tag{4.32}$$

where $k_{\max}(t)$ is the maximum wave vector to which the concentration cascade has penetrated. Since this cascade is purely passive for $t < t_c$, we have

$$C(k,t) = C(k_0)(k/k_0)^{-5/3}, \quad k < k_{\max}(t) \tag{4.33}$$

where concentration fluctuations are initially present in the vicinity of k_0. Conservation of total concentration implies that the amplitude $C(k_0)$ is approximately independent of time at the short times of interest here. Upon equating $k_{\max}(t_c)$ with k_c, Eqs. (4.34) and (4.33) may be combined to give the stretching of $(\nabla\psi_{\rm rms})$

$$[\nabla\psi(t_c)]_{\rm rms} \approx \left(\frac{k_c}{k_0}\right)^{2/3}[\nabla\psi(0)]_{\rm rms}\,. \tag{4.34}$$

Inserting this estimate in Eq. (4.31), we find finally

$$k_c = \epsilon^{1/3}k_0^{2/3}/\alpha^{1/2}[\nabla\psi(0)]_{\rm rms}\,. \tag{4.35}$$

The formula (4.35) is in excellent agreement with our numerical simulations of the closure equations for $\alpha = 1$. For realistic values of α, we find that k_c always *exceeds* k_d, indicating that concentration waves are in fact unimportant in the inertial range. The estimate $\alpha \sim \nu^2$, together with $[\vec{\nabla}\psi(0)]_{\rm rms} \sim k_0$, leads to

$$\frac{k_c}{k_d} = \left(\frac{k_d}{k_0}\right)^{1/3} \gg 1\,, \tag{4.36}$$

supporting the same conclusion. Although formulas (4.30b) and (4.35) do not apply to real mixtures, we expect that they can be taken over to the persistent vector-potential fluctuations observed by Pouquet[20] in two-dimensional MHD.

V. WAVE EFFECTS IN THE VISCOUS-CONVECTIVE RANGE

As we have seen, real binary mixtures behave like "passive" mixtures in the inertial range between k_0 and k_d. However, the viscous-convective range of wave vectors in high-Prandtl-number fluids can be shortened considerably by wave effects. Concentration gradients for $k \gg k_d$ are simply transformed into velocity fluctuations and dissipated.

To understand this effect more quantitatively, consider the exact concentration wave dispersion relation arising from (3.28), namely

$$\omega_\pm(k) = \pm\tfrac{1}{2}[4\alpha B^2k^2 - (D-\nu)^2k^4]^{1/2} - \tfrac{1}{2}i(D+\nu)k^2\,. \tag{5.1}$$

The quantity B_0 has been replaced by the root-mean-square concentration gradient due to scales larger than k^{-1}, namely,

$$B(k) \equiv \left(\int_0^k k^2 C(k)\,dk\right)^{1/2}. \tag{5.2}$$

Taking over estimates discussed in Sec. IV, we have, for $k < k_d$,

$$B(k) = B(k_0)(k/k_0)^{2/3}\,. \tag{5.3}$$

Remembering that $\alpha \sim \nu^2$ and noting that $B(k_0) \sim k_0$, we can construct a wave time

$$\tau_w(k) = 1/\sqrt{\alpha}\,B(k) \sim 1/\nu k^{5/3}k_0^{1/3}\,, \tag{5.4}$$

which must be compared to the diffusive times $1/\nu k^2$ and $1/Dk^2$. For high-Prandtl-number mixtures, $1/\nu k^2$ is always shorter than either $1/Dk^2$ or $\tau_w(k)$. However, the wave time is itself shorter than $1/Dk^2$ for all wave vectors less than

$$k' = (\nu/D)^3k_0\,. \tag{5.5}$$

Since k' far exceeds k_d in typical turbulent mixtures, we are justified in neglecting Dk^2 in Eq. (5.1), and expanding in $1/\tau_w$. The resulting eigenfrequencies are

$$\omega_+ \approx -i\nu k^2, \quad \omega_- \approx -i\alpha B^2(k)/\nu\,, \tag{5.6}$$

with ω_+ corresponding essentially to pure velocity fluctuations, and ω_- primarily relaxing concentration fluctuations.

Although the concentration has acquired a new damping mechanism from the "waves," the damping rate ω_- is still negligible compared to the turbulent eddy turnover time even at k_d. Thus, the $C(k) \sim k^{-1}$ viscous-convective range discussed in Sec. III B will be established beyond k_d, just as in passive mixtures. Now, however, the cascade will be cut off when ω_- reaches the random strain rate $t_d^{-1} \sim \nu k_d^2$ [see (3.22)]. Neglecting possible logarithmic corrections, we find that in the viscous-convective range,

$$B(k) = B(k_d)\left(\frac{k}{k_d}\right)^2 = B(k_0)\left(\frac{k_d}{k_0}\right)^{2/3}\left(\frac{k}{k_d}\right)^2. \tag{5.7}$$

Equating ω_- and t_d^{-1}, we find the viscous-convective range terminates beyond a wave vector

$$k^* = k_d(k_d/k_0)^{1/3}\,. \tag{5.8}$$

Concentration fluctuations will persist out to k^*, provided k_d is not so large that passive scalar cutoff $k_d' = \sqrt{\nu/D}\,k_d$ does not come in first. It appears

that overdamped "waves" will dominate in limiting the viscous-convective range for high-Prandtl-number mixtures at Reynolds numbers accessible in the laboratory.

VI. TURBULENCE IN PHASE-SEPARATING BINARY MIXTURES

As mentioned in the Introduction, turbulence in the two-phase region of Fig. 1 raises some intriguing questions. To treat this unstable regime correctly, one must generalize the model of symmetric binary mixtures defined by Eqs. (1.8) and (1.9). Although the equation for the time evolution of the velocity is unchanged (except for a modification of the pressure), Eq. (1.8) becomes[13,14]

$$\partial_t \psi + (\vec{v}\cdot\vec{\nabla})\psi = \lambda\nabla^2 \frac{\delta \mathfrak{F}}{\delta \psi}\,, \tag{6.1}$$

where λ is a positive transport coefficient, and the functional derivative is of an effective long-wavelength free energy

$$\mathfrak{F} = \left(\frac{k_B T}{\xi^3}\right)\int d^3x\left(\tfrac{1}{2}\xi^2\left|\vec{\nabla}\psi\right|^2 + \tfrac{1}{2}r\psi^2 + u\psi^4\right). \tag{6.2}$$

The parameter u is usually taken to be positive and temperature independent while (according to mean field theory) r changes sign at T_c,

$$r \propto T - T_c\,. \tag{6.3}$$

The quantity ξ is a correlation length which sets the scale of the coarse graining needed to produce (6.2). Well above T_c, we can neglect both the quartic coupling and gradient term in (6.2), and recover the simple convective equation (1.8), with

$$D \equiv D_0 = \lambda k_B T_c/\xi^3\,. \tag{6.4}$$

When mixtures in equilibrium above T_c are suddenly quenched into the two-phase region (see Fig. 1) a dynamic instability occurs.[38] If concentration fluctuations are small initially, we can neglect the quartic coupling in (6.2) and write (6.1) in Fourier space as[38]

$$\partial_t \psi_k + N = -\,D(k)k^2\psi_k\,, \tag{6.5}$$

with

$$D(k) = -\,|D_0| + (\lambda k_B T/\xi)k^2\,, \tag{6.6}$$

where N is a nonlinear term. Since $r<0$ below T_c, $D_0 = \lambda k_B\,\mathrm{Tr}/\xi^2$ is *negative*, as is $D(k)$ for small enough k. According to (6.5), concentration fluctuations will be amplified with a maximum growth rate occurring at

$$\bar{k}^2 = |D_0|\,\xi/2\lambda k_B T\,. \tag{6.7}$$

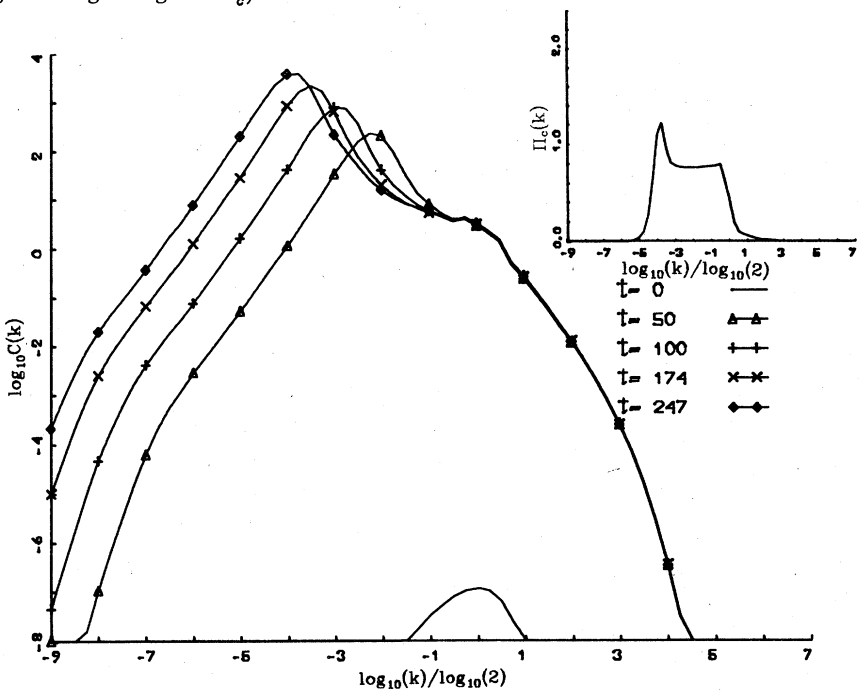

FIG. 14. The inverse cascade of concentration fluctuations obtained by introducing a random forcing in Eq. (1.8). The spectrum of both the concentration and the kinetic forcing peak at $k \equiv k_0 \simeq 1$, and are normalized such that $\int_0^\infty F_v(k)dk = \int_0^\infty F_c(k)dk = 1$. The initial conditions are $E_v(k, t=0) = C(k, t=0) = 0$. The viscosity is $\nu = 6\times 10^{-3}$ and the Prandtl number is $P = 1$. Time is measured in units of the velocity turnover time at $k = k_0$. The inset shows $\Pi_c(k)$ at time $t = 247$. The lack of linearity of the concentration spectrum in the region where $\Pi_c(k)$ is k independent is a consequence of the waves trying to produce equipartition between $C(k)$ and $2k^2C(k)$. The peaks of $C(k)$ at different times line up, however, with a $\frac{7}{3}$ slope.

The wave vector k_{max} determines the initial size of droplets of A and B phase which form from the uniform mixture and then coarsen.[39] Experimentally, laser light scattering experiments reveal a striking ring-shaped intensity pattern (with a radius of order $\bar{k}^{-1}$), which shrinks in time as the mixture coarsens.[9]

The negative diffusion constant appearing in (6.5) injects concentration fluctuations at wavelengths comparable to $\bar{k}^{-1}$, which can be of the order of several thousand angstroms.[9] The conditions are then ideal for the inverse cascade of concentration fluctuations discussed in Secs. II and III of this paper: If appropriate equilibrium Langevin noise sources act on (1.9) and (6.1), it is straightforward to show (neglecting the quartic coupling) that the system relaxes toward a distribution function of the form (2.5), with

$$B = r < 0 . \tag{6.8}$$

As we have seen, a negative B is associated with a possible inverse cascade.

An inverse cascade is already contained in the closure equations (4.2)–(4.5). In Fig. 14, we show the result of artificially injecting concentration fluctuations by adding a random force to the right-hand side of (1.8) with $\alpha = 1$. There is a time-dependent infrared cascade of concentration fluctuations with the spectrum predicted by (3.32),

$$C(k) \sim k^{-7/3} . \tag{6.9}$$

Although the conditions in real mixtures are different from those in Fig. 14, we expect that a related inverse cascade may in fact appear at intermediate times in phase-separating binary mixtures. Of course, the quartic term in (6.2) ultimately becomes important for stability during the late stages of phase separation. Equation (6.2) then acquires a third-order nonlinearity and our analysis must be revised.

Complete phase separation can be prevented if the mixtures are stirred violently at long wavelengths. The Kolmogorov cascade of velocity fluctuations toward short length scales will mix the phase-separating fluid when it collides with the inverse cascade mentioned above. For large Reynolds numbers, an unusual steady state should develop. We hope to investigate this problem using the closure and phenomenological ideas developed here in a future publication.

ACKNOWLEDGMENTS

It is a pleasure to thank U. Frisch both for fruitful conversations and stimulating lectures on modern turbulence theory given at Harvard. We have also benefited from discussions with B. I. Halperin, P. C. Martin, A. Pouquet, and W. Press. This work was supported by the National Science Foundation under Grant No. DMR77-09595. One of us (RR) would like to acknowledge the Fundación I.T.P., Madrid, Spain for financial support, and the hospitality from Harvard University. DRN acknowledges the receipt of a grant from the Alfred P. Sloan Foundation.

APPENDIX A: "ASYMMETRIC" BINARY MIXTURES AND ESTIMATE OF α

Real binary mixtures do not have a special symmetry which ensures that concentration and thermal diffusion decouple. Although such a symmetry is implicit in Eqs. (1.8) and (1.9), it is not difficult to generalize the model.[13] Again, assuming characteristic velocities much less than the sound speed, the equations of motion are[13]

$$\partial_t \psi_1 + (\vec{v}\cdot\vec{\nabla})\psi_1 = D\nabla^2\psi_1 + L_1\nabla^2\psi_2 , \tag{A1}$$

$$\partial_t \psi_2 + (\vec{v}\cdot\vec{\nabla})\psi_2 = \kappa\nabla^2\psi_2 + L_2\nabla^2\psi_1 , \tag{A2}$$

$$\partial_t \vec{v} + (\vec{v}\cdot\vec{\nabla})\vec{v} = -\frac{1}{\rho_0}\vec{\nabla}p - \alpha\vec{\nabla}\psi_1\nabla^2\psi_1 - \beta\vec{\nabla}\psi_2\nabla^2\psi_2 + \nu\nabla^2\vec{v} + \vec{f} , \tag{A3a}$$

$$\vec{\nabla}\cdot\vec{v} = 0 . \tag{A3b}$$

We take ψ_1 to be the concentration variable (1.7) and form ψ_2 from a linear combination of entropy and concentration fluctuations. The linear combination is chosen so that the absolute equilibrium probability distribution in Fourier space is just[13]

$$\mathcal{P}(\{\vec{v}_{\vec{k}}\},\{\psi_1(\vec{k})\},\{\psi_2(\vec{k})\}) \propto \exp\left(-\tfrac{1}{2}\sum_{\vec{k}}\{A[|\vec{v}_k|^2 + \alpha k^2|\psi_1(\vec{k})|^2 + \beta k^2|\psi_2(\vec{k})|^2]\} + B|\psi_1(\vec{k})|^2 + C|\psi_2(k)|^2\right), \tag{A4}$$

where A, B, and C are constants and, of course,

$$\vec{k}\cdot\vec{v}_k \equiv 0 . \tag{A5}$$

There is no cross coupling between ψ_1 and ψ_2. This equilibrium distribution is associated with the conservation of the squared integrals of ψ_1 and ψ_2, as well as of E_{tot} defined by (2.9) in the absence of forcing and dissipation. If ψ_2 is allowed to relax to zero in (A1)–(A3), one recovers the model of "symmetric" binary mixtures studied in this paper.

Taking over the analysis of Sec. II, we see that

inverse cascades in both $\psi_1(k)$ and $\psi_2(k)$ are possible. As discussed in Sec. VI, one might expect an inverse cascade of concentration fluctuations in the two-phase region of Fig. 1 where B is negative. If the mixture is above its consolute point, it could still be near an ordinary liquid-gas critical point, described by the order parameter ψ_2.[13] Well within the region of two-phase liquid-gas coexistence, C would be negative and an inverse cascade of ψ_2 is possible.

Model parameters like α and β can be estimated by appealing to absolute equilibrium. Returning to symmetric binary mixtures, we can estimate α by noting that the equilibrium probability distribution above T_c should be of the form

$$\mathcal{P} \propto e^{-F/k_B T} \tag{A6}$$

with [compare with (6.2)]

$$F = \xi^{-3} \int d^3 r \left(\tfrac{1}{2} m |\vec{v}|^2 + \tfrac{1}{2} \chi^{-1} \xi^2 |\vec{\nabla} \psi|^2 + \tfrac{1}{2} \chi^{-1} \psi^2 \right). \tag{A7}$$

Here, m is the particle mass, ξ is the correlation length, and χ is concentration susceptibility. Comparison with (2.5a) gives immediately

$$\alpha(T) = \xi^2(T)/m\chi(T). \tag{A8}$$

Here we work in the mean-field approximation, where

$$\xi(T) \sim \frac{1}{|T - T_c|^{1/2}}, \quad \chi(T) \sim \frac{1}{|T - T_c|}, \tag{A9}$$

so α is approximately temperature independent.

Evaluating α far above T_c for convenience, we take $\chi(T)$ to be the concentration susceptibility of an "ideal" binary mixture[40]

$$\chi(T) = 1/k_B T. \tag{A10}$$

In this same limit we expect the fluid shear viscosity to be of order of an interparticle separation times a typical particle velocity,

$$\nu \sim \xi \left(\frac{k_B T}{m} \right)^{1/2}. \tag{A11}$$

Inserting (A10) into (A8), we have finally

$$\alpha \sim \nu^2. \tag{A12}$$

Note that α is not related to the mixture concentration diffusivity, which *vanishes* near T_c.

APPENDIX B: DERIVATION OF CLOSURE EQUATIONS

We summarize briefly in this appendix the steps needed to derive the spectral equations (4.2) to (4.5). One begins by writing Eqs. (1.8) to (1.9) in Fourier space:

$$(\partial_t + \nu k^2) u_i(k) = -\frac{i}{2} P_{ijl}(k) \sum_{k=p+q} v_j(p) v_l(q) + \frac{i\alpha}{2} P_{ij}(k) \sum_{k=p+q} \psi(p)\psi(q) q_j (p^2 - q^2), \tag{B1}$$

$$(\partial_t + Dk^2)\psi(k) = -i \sum_{k=p+q} \vec{q} \cdot \vec{u}(p) \psi(q), \tag{B2}$$

where

$$u_i(k) = P_{ij}(k) v_j(k), \tag{B3}$$

$$P_{ijl}(k) = k_j P_{il}(k) + k_l P_{ij}(k), \tag{B4}$$

and $P_{ij}(k)$ is the transverse projector

$$P_{ij}(k) = \delta_{ij} - \frac{k_i k_j}{k^2}. \tag{B5}$$

It is very convenient to introduce a self-explanatory and more compact notation in which Eqs. (B1) and (B2) read

$$\partial_t v_1 = \gamma_{123} v_2 v_3 + \delta_{123} \psi_2 \psi_3 + L^v_{12} v_2 + f_1, \tag{B6}$$

$$\partial_t \psi_1 = \beta_{123} v_2 \psi_3 + L^D_{12} \psi_2. \tag{B7}$$

The subscripts in (B6) and (B7) represent both vector indices and Fourier components, and a summation convention compatible with conservation of momentum is assumed. The vertices γ, β, δ, L^v, L^D are defined by comparison between (B6), (B7) and (B1), (B2).

To obtain the hierarchy of cumulants with maximum economy in the algebra, we introduce two auxiliary fields ρ and ϕ, and define the moment generating functional as

$$Z = \langle e^{i\rho_1 v_1 + i\phi_1 \psi_1} \rangle. \tag{B8}$$

Averages can be obtained from Z by differentiation:

$$\langle v_{i_1} v_{i_2}, \ldots, v_{i_n} \psi_{j_1}, \ldots, \psi_{j_m} \rangle = \frac{1}{i^{n+m}} \frac{\delta^{n+m} Z}{\delta \rho_{i_1}, \ldots, \delta \rho_{i_n} \delta \phi_{j_1}, \ldots, \delta \phi_{j_n}} \Big|_{\phi = \rho = 0}. \tag{B9}$$

Using (B6) and (B7) we obtain for Z the equation

$$\frac{\partial Z}{\partial t} = \left[i\rho_1 \left(\frac{\gamma_{123}}{i^2} \frac{\delta^2}{\delta\rho_2 \delta\rho_2} + \frac{\delta_{123}}{i^2} \frac{\delta^2}{\delta\phi_2 \delta\phi_3} \right) + i\phi_1 \frac{\beta_{123}}{i^2} \frac{\delta^2}{\delta\rho_2 \delta\phi_3} \right] Z, \tag{B10}$$

where we have omitted the linear terms that do not pose any closure problem. It is more convenient to work with a functional H;

$$H = \ln Z, \tag{B11}$$

that generates the statistical cumulants. H obeys the equation

$$\frac{\partial H}{\partial t}=i\phi_1\left[\frac{\gamma_{123}}{i^2}\left(\frac{\delta^2 H}{\delta\rho_2\delta\rho_3}+\frac{\delta H}{\delta\rho_2}\frac{\delta H}{\delta\rho_3}\right)+\frac{\delta_{123}}{i^2}\left(\frac{\delta H}{\delta\phi_2\delta\phi_3}+\frac{\delta H}{\delta\phi_2}\frac{\delta H}{\delta\phi_3}\right)\right]$$
$$+i\phi_1\left[\frac{\beta_{123}}{i^2}\left(\frac{\delta^2 H}{\delta\rho_2\delta\phi_3}+\frac{\delta H}{\delta\rho_2}\frac{\delta H}{\delta\phi_3}\right)\right]. \tag{B12}$$

The equations of motion for the cumulants are now obtained by functional differentiation of (B12). The results that we need are

$$\partial_t\langle\psi_1\psi_2\rangle=1/i^2\frac{\delta^2 H}{\delta\phi_1\delta\phi_2}\Big|_{\phi=\rho=0}=\beta_{134}\langle\psi_2\psi_4 v_3\rangle_c+\beta_{234}\langle\psi_1\psi_4 v_3\rangle_c, \tag{B13}$$

$$\partial_t\langle v_1 v_2\rangle=\gamma_{134}\langle v_2 v_3 v_4\rangle_c+\gamma_{234}\langle v_1 v_3 v_4\rangle_c+\delta_{134}\langle v_2\psi_3\psi_4\rangle_c+\delta_{234}\langle v_1\psi_3\psi_4\rangle_c, \tag{B14}$$

$$\partial_t\langle v_1\psi_2\psi_3\rangle=\gamma_{145}(\langle v_4 v_5\psi_2\psi_3\rangle_c+2\langle v_4\psi_2\rangle\langle\psi_3 v_5\rangle)+\delta_{145}(\langle\psi_2\psi_3\psi_4\psi_5\rangle_c+2\langle\psi_2\psi_4\rangle\langle\psi_3\psi_5\rangle)$$
$$+\beta_{245}(\langle v_1 v_4\psi_3\psi_5\rangle_c+\langle v_1 v_4\rangle\langle\psi_3\psi_5\rangle+\langle v_1\psi_5\rangle\langle v_4\psi_3\rangle)+\beta_{345}(\langle v_1 v_4\psi_2\psi_5\rangle+\langle v_1 v_4\rangle\langle\psi_2\psi_5\rangle+\langle v_1\psi_5\rangle\langle v_4\psi_2\rangle), \tag{B15}$$

where the symbol $\langle\ \rangle_c$ means statistical cumulant. For example,

$$\langle v_1 v_2 v_3\rangle_c=\langle v_1 v_2 v_3\rangle-\langle v_1\rangle\langle v_2 v_3\rangle-\langle v_2\rangle\langle v_1 v_3\rangle-\langle v_3\rangle\langle v_1 v_2\rangle. \tag{B16}$$

One now carries out a short-time expansion[1] of Eqs. (B13) and (B15), and assumes Gaussian statistics at $t=0$. We write, for example,

$$\frac{\partial}{\partial t}\langle v_1 v_2(t)\rangle=\frac{\partial}{\partial t}\langle v_1 v_2(t)\rangle|_{t=0}+t\frac{\partial^2}{\partial t^2}\langle v_1 v_2(t)\rangle|_{t=0}. \tag{B17}$$

In this way, one finds

$$\partial_t\langle v_1 v_2(t)\rangle=4t(\gamma_{134}\gamma_{256}\langle v_3 v_5\rangle\langle v_4 v_6\rangle+2\gamma_{134}\gamma_{356}\langle v_2 v_5\rangle\langle v_4 v_6\rangle+\delta_{134}\delta_{256}\langle c_3 c_5\rangle\langle c_4 c_6\rangle+\delta_{134}\beta_{356}\langle v_2 v_5\rangle\langle c_4 c_6\rangle), \tag{B18}$$

$$\partial_t\langle c_1 c_2(t)\rangle=2t(2\beta_{134}\delta_{356}\langle c_2 c_5\rangle\langle c_4 c_6\rangle+\beta_{134}\beta_{256}\langle v_3 v_5\rangle\langle c_4 c_6\rangle+\beta_{456}\beta_{134}\langle v_3 v_5\rangle\langle c_2 c_6\rangle). \tag{B19}$$

These equations are, of course, exact in the limit $t\to 0$. Returning to the notation of (B1) and (B2), one obtains after considerable algebra

$$\partial_t C_{(k)}=T_c(k) \tag{B20}$$

and

$$\partial_t E_v(k)=T_v(k), \tag{B21}$$

where

$$T_c(k)=\frac{4S_{d-1}}{S_d}\,t\int_{\Delta_k}\int dp\,dq\left(\frac{\sin\beta}{k}\right)^{d-1}\frac{kq}{p}\left(\frac{E_v(p)}{d-1}\left[k^{d-1}C(q)-q^{d-1}C(k)\right]-\alpha(k^2-q^2)p^2C(k)C(q)\right) \tag{B22}$$

and

$$T_v(k)=\frac{8S_{d-1}}{S_d}\,t\int_{\Delta_k}\int dp\,dq\left(\frac{\sin\beta}{k}\right)^{d-3}\frac{1}{kpq}\left[\frac{k^2}{(d-1)^2}\,b_{kpq}E_v(q)[k^2E_v(p)-p^2E_v(k)]\right.$$
$$\left.+\frac{\sin^2\beta}{k^2}\,p^2q^2(p^2-q^2)\left(\frac{\alpha^2}{4}(p^2-q^2)k^{d-1}C(p)C(q)-\frac{\alpha}{2(d-1)}\,p^2C(q)E_v(k)\right)\right]. \tag{B23}$$

These expressions are identical to (4.4) and (4.5) in $d=3$, with the replacements

$$\theta^{(i)}_{kpq}(t)\to t. \tag{B24}$$

The more elaborate expressions (4.7) agree with (B24) in the limit $t\to 0$. The detailed motivation for choosing triad relaxation times as in (4.7) is discussed in Ref. 1. Most of our results depend only on the triad relaxation times satisfying

$$\theta^{(i)}_{kpq}(t)\underset{t\to 0}{\to}t,\qquad \theta^{(i)}_{kpq}(t)\underset{t\to\infty}{\to}1/\mu^{(i)}_{kpq} \tag{B25}$$

(see Appendix C). The basic assumption is a

rapid loss of memory ("stochastic scrambling") of the turbulent cumulants.

APPENDIX C: SPECTRAL EXPONENTS

We describe in this appendix how to obtain the results that we earlier summarized in Table I. Mathematically, the inertial range spectra are required to satisfy

$$T_c(k)=T_v(k)=0\,, \tag{C1}$$

where $T_c(k)$ and $T_v(k)$ are given by (4.4) and (4.5). A method which allows us to extract power-law solutions from (C1) has been given by Orszag.[1] We assume that there exists an inertial range where

$$\begin{aligned}&\theta_{kpq}\sim\theta_{kkk}\sim k^{-a}\,,\\ &E_p\sim p^{-m}\,,\\ &C_q\sim q^{-n}\,.\end{aligned} \tag{C2}$$

The change of variables

$$\begin{aligned}&(k,p,q)\to(k,p,\sigma)=(k/\sigma)(\sigma,p,k)\,,\\ &dp\,dq=(k/\sigma)^3dp\,dq\end{aligned} \tag{C3}$$

leads to

$$\begin{aligned}T_Q(k)&=\int_{\Delta_k}\int dp\,dq\;T_Q(k\,|pq)\\ &=\int\int dp\,d\sigma(k/\sigma)^{e(a,m,n)}T_Q(k\,|pq)\,,\end{aligned} \tag{C4}$$

where Q is either C or v and $e(a,m,n)$ is a polynomial of first degree in a,m,n. We then choose values of a,m,n such that $e\equiv0$, thereby obtaining

$$\begin{aligned}T_Q(k)&=\int\int dp\,d\sigma\;T_Q(k\,|p\sigma)\\ &=\int\int dp\,d\sigma\;T_Q(\sigma\,|pk)\,.\end{aligned} \tag{C5}$$

Symmetrizing and using the detailed balance conditions (4.11) and (4.12) we see immediately that (C1) is satisfied. Thus, to obtain the inertial range exponents, one just has to solve

$$e(a,m,n)=0\,. \tag{C6}$$

Equations (4.7) to (4.9) for the triad relaxation times lead to additional relations between a,m, and n:

(i) In the regimes where it is legitimate to neglect the contribution proportional to C_w in (4.9), we have

$$a=\frac{3-n}{2}\,. \tag{C7}$$

(ii) In the wave-dominated regimes is the term proportional to C_E which is negligible. Therefore,

$$a=1\,. \tag{C8}$$

The solution of (C6) with the restrictions (C7), (C8) yields the results of Table I. To get information about the cascades from (4.2)–(4.6), recall from Sec. IV B that we say that there is a cascade of a quantity Q if the flux

$$\pi_Q(k)=\int_0^k T_Q(q)dq \tag{C9}$$

is independent of k (for wave numbers in the inertial range). This is equivalent to saying that there is a range of values of a real constant λ such that

$$\int_0^k dq\;T_Q(q)=\int_0^{\lambda k}dq\;T_Q(q)\,, \tag{C10}$$

which implies, after an obvious change of variables in the second integral,

$$T_Q(\lambda k\,|\lambda p,\lambda q)=1/\lambda^3T_Q(k\,|p,q)\,. \tag{C11}$$

It is very easy to check that (C11) together with (C2) is equivalent to (C6).

APPENDIX D: SELF-CONSISTENT DETERMINATION OF THE WAVE PART OF THE TRIAD RELAXATION TIME

The wave contribution to the spectral equations of motion is [see (4.28a) and (4.28b)]

$$\begin{aligned}&(\partial_t E_k^v)_{\rm LS}=\alpha k^2\Gamma_k(\alpha k^2C_k-E_k^v/2)\,,\\ &(\partial_t k^2C_k)_{\rm LS}=k^2\Gamma_k(E_k^v/2-\alpha k^2C_k)\,,\end{aligned} \tag{D1}$$

where

$$\Gamma_k=\frac{8}{3}\left(\int_0^k dq\,\theta_{kkq}q^2C(q)\right). \tag{D2}$$

This shows that relaxation to equipartition takes place in a time of order

$$\theta^{-1}=\tfrac{3}{2}k^2\Gamma_k\,. \tag{D3}$$

Since it follows from (4.7) that

$$\theta_{kkq}^{-1}\simeq2\mu_k\,, \tag{D4}$$

we can combine (D2) with (D3) and find

$$\theta_{kkq}^{-2}\simeq k^2\int_0^k dq\,q^2C(q)\,. \tag{D5}$$

This suggests we set $C_w\equiv1$ in Eq. (4.9).

APPENDIX E: HYDRODYNAMIC SINGULARITIES IN THE MARKOVIAN RANDOM-COUPLING MODEL

We present here the derivation of (4.17). We start from the Markovian random-coupling-model version of Eq. (4.3) with $\alpha\equiv0$, namely,

$$\partial_t k^2 C_k = \frac{4S_{d-1}}{S_d}\theta_0 \int_{\Delta_k}\int dp\,dq \left(\frac{\sin\beta}{k}\right)^{-1}\frac{k^3 q}{p} \times \frac{E_p}{d-1}\left(k^{d-1}C_q - q^{d-1}C_k\right). \quad \text{(E1)}$$

Integrating over k, and recalling the definition

$$E_G = \int_0^\infty dk\, k^2 C_k, \quad \text{(E2)}$$

we obtain, after some simple manipulations,

$$\frac{d}{dt}E_G = \frac{4S_{d-1}}{(d-1)S_d}\theta_0 \int\int_\Delta\int dk\,dp\,dq\,(\sin\beta)^{d-1} \times \frac{kq}{p}E_p C_q (k^2 - q^2). \quad \text{(E3)}$$

Introducing polar coordinates with β as the aximuthal angle, all the integrations can be done explicitly, with the result

$$\frac{d}{dt}E_G = \frac{4S_{d-1}}{(d-1)S_d}\theta_0 \frac{\Gamma(\frac{1}{2})\Gamma(d+\frac{1}{2})}{\Gamma[(d+2)/2]}\Omega(t)E_G. \quad \text{(E4)}$$

The enstrophy Ω is defined by Eq. (4.16). The derivation of Eq. (4.17) from (4.2) is very similar, and can be found in Appendix 4 of the review by Rose and Sulem.

Similar, but more complicated equations can also be derived for $E_G(t)$ and $\Omega(t)$ for $\alpha \neq 0$. They suggest the sharp onset of dissipation shown in Fig. 13. The results are analogous to those of Pouquet[20] for MHD turbulence.

[1]For reviews of modern turbulence theory, see H. A. Rose and P.-L. Sulem, J. Phys. (Paris) 39, 44 (1978); S. A. Orszag, in *Fluid Dynamics*, Proceedings of the 1973 Les Houches Summer School, edited by R. Balian and P. L. Peube (Gordon and Breach, New York, 1977).

[2]A. N. Kolmogorov, C. R. Acad. Sci. USSR 30, 301 (1941); see also Usp. Fiz. Nauk 93, 476 (1967) [Sov. Phys.—Usp. 10, 734 (1968)].

[3]A. M. Obukhov, Izv. Akad. Nauk SSSR, Georgr. Geofiz. 13, 58 (1949).

[4]S. Corrsin, J. Appl. Phys. 22, 469 (1951).

[5]G. K. Batchelor, J. Fluid Mech. 5, 113 (1959).

[6]R. H. Kraichnan, Phys. Fluids 11, 945 (1968).

[7]R. H. Kraichnan, Phys. Fluids 13, 22 (1970).

[8]R. H. Kraichnan, J. Fluid Mech. 64, 737 (1974).

[9]See, e.g., W. I. Goldburg and J. S. Huang, in *Fluctuations, Instabilities and Phase Transitions*, edited by T. Riste (Plenum, New York, 1975).

[10]See, e.g., W. J. Cocke, Phys. Fluids 12, 2488 (1969); S. A. Orszag, *ibid.* 13, 2203 (1970).

[11]L. P. Kadanoff and J. Swift, Phys. Rev. 166, 89 (1968); J. Swift, *ibid.* 173, 257 (1968).

[12]K. Kawasaki, Ann. Phys. (N. Y.) 61, 1 (1970).

[13]E. D. Siggia, B. I. Halperin, and P. C. Hohenberg, Phys. Rev. B 13, 2110 (1976).

[14]P. C. Hohenberg and B. I. Halperin, Rev. Mod. Phys. 49, 43 (1977), and references therein.

[15]L. D. Landau and I. M. Lifshitz, *Fluid Mechanics* (Pergamon, London, 1959).

[16]R. H. Morf, S. A. Orszag, and U. Frisch, Phys. Rev. Lett. 44, 572 (1980).

[17]We are indebted to U. Frisch for this observation.

[18]R. H. Kraichnan, Phys. Fluids 8, 1385 (1965).

[19]A. Pouquet, U. Frisch, and J. Léorat, J. Fluid Mech. 77, 321 (1976).

[20]A. Pouquet, J. Fluid Mech. 88, 1 (1978).

[21]U. Frisch, A. Pouquet, J. Léorat, and A. Mazure, J. Fluid Mech. 68, 769 (1975).

[22]J. Lighthill, *Waves in Fluids* (Cambridge University Press, New York, 1979), Chap. IV.

[23]The argument is identical to one used by Kraichnan in Ref. 18 for MHD turbulence.

[24]This technique was first used to predict an inverse cascade of kinetic energy in two-dimensional Navier-Stokes turbulence: R. H. Kraichnan, Phys. Fluids 10, 1417 (1967).

[25]U. Frisch, A. Pouquet, J. Léorat, and A. Mazure, J. Fluid Mech. 65, 145 (1974).

[26]D. Fyfe and D. Montgomery, J. Plasma Phys. 16, 181 (1976).

[27]V. N. Desnyansky and E. A. Novikov, Prinkl. Mat. Mekh. 38, 507 (1974); V. N. Desnyansky and E. A. Novikov, Atmos. Oceanic Phys. 10, 127 (1974); T. L. Bell and M. Nelkin, Phys. Fluids 20, 345 (1977); J. Fluid Mech. 88, 369 (1978); E. D. Siggia, Phys. Rev. A 17, 1166 (1978); R. M. Kerr and E. D. Siggia, J. Stat. Phys. 19, 543 (1978).

[28]Kovaznay, J. Aeronaut. Sci. 15, 745 (1948).

[29]J. Leith, Phys. Fluids 10, 1409 (1967).

[30]See, e. g., J. D. Jackson, *Classical Electrodynamics* (Wiley, New York, 1967); L. D. Landau and I. M. Lifshitz, *Electrodynamics of Continuous Media* (Pergamon, New York, 1975).

[31]A. Pouquet, M. Lesieur, J. C. Andrê, and C. Basdevant, J. Fluid Mech. 72, 305 (1975).

[32]J. C. Andrê and M. Lesieur, J. Fluid Mech. 81, 187 (1977).

[33]Using arguments similar to those used to prove Boltzmann's *H* theorem, it is possible to show rigorously that bounded spectra obeying closure equations approach absolute equilibrium at long times. See G. Carnevale, Ph. D. Harvard thesis, 1977 (unpublished).

[34]C. Leith, J. Atmos. Sci. 28, 145 (1971).

[35]U. Frisch, M. Lesieur, and A. Brissaud, J. Fluid Mech. 65 145, (1974).

[36]M. Lesieur and D. Shertzer, J. Mec. 17, 610 (1978).

[37]L. F. Richardson, Proc. R. Soc. London, Ser. A 110, 709 (1926).

[38]See, e.g., J. S. Langer, in *Fluctuations, Instabilities, and Phase Transitions*. edited by T. Riste (Plenum, New York, 1975), and references therein.

[39]The initial coarsening in symmetric binary mixtures has been studied by K. Kawasaki and T. Ohta, Prog. Theor. Phys. 59, 362 (1978).

[40]See, e.g., D. A. McQuarrie, *Statistical Mechanics* (Harper and Row, New York, 1976).